Dissertation VTT PUBLICATIONS 772

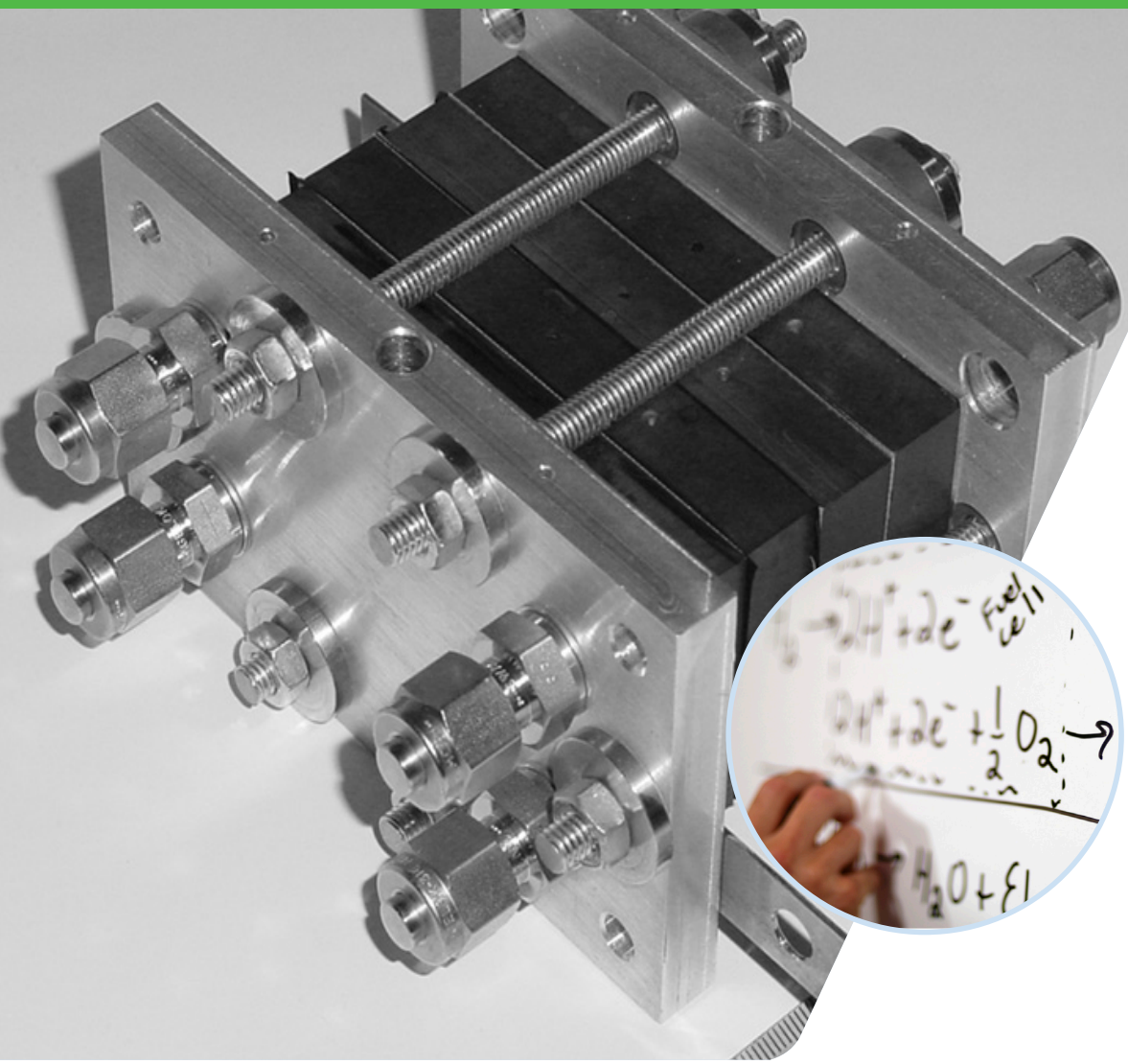

Suvi Karvonen

Modelling approaches to mass transfer and compression effects in polymer electrolyte fuel cells

VTT PUBLICATIONS 772

Modelling approaches to mass transfer and compression effects in polymer electrolyte fuel cells

Suvi Karvonen

Doctoral dissertation for the degree of Doctor of Science in Technology (Doctor of Philosophy) to be presented with due permission of the School of Science for public examination and debate in Auditorium K216 (Otakaari 4) at the Aalto University School of Science (Espoo, Finland) on the 25th of November 2011 at 12 noon.

ISBN 978-951-38-7754-5 (soft back ed.)
ISSN 1235-0621 (soft back ed.)

ISBN 978-951-38-7755-2 (URL: http://www.vtt.fi/publications/index.jsp)
ISSN 1455-0849 (URL: http://www.vtt.fi/publications/index.jsp)

JULKAISIJA – UTGIVARE – PUBLISHER

VTT, Vuorimiehentie 5, PL 1000, 02044 VTT
puh. vaihde 020 722 111, faksi 020 722 4374

VTT, Bergsmansvägen 5, PB 1000, 02044 VTT
tel. växel 020 722 111, fax 020 722 4374

VTT Technical Research Centre of Finland, Vuorimiehentie 5, P.O. Box 1000, FI-02044 VTT, Finland
phone internat. +358 20 722 111, fax + 358 20 722 4374

Kopijyvä Oy, Kuopio 2011

Suvi Karvonen. Modelling approaches to mass transfer and compression effects in polymer electrolyte fuel cells [Polymeerielektrolyyttipolttokennojen massansiirron ja puristuspaineen vaikutusten mallintaminen]. Espoo 2011. VTT Publications 772. 73 p. + app. 66 p.

Keywords PEMFC, fuel cell, modelling

Abstract

The subject of this thesis is modelling polymer electrolyte membrane fuel cells (PEMFCs) locally and on a cell scale. The modelling was done using software based on the finite element method and focused on mass transfer issues and compression pressure distribution and its effects on local phenomena.

Mass transfer, more specifically the flow distribution in the flow field system, was studied on the cathode. The velocity distribution was improved by changing the geometry of the channel system. This improvement was also observed experimentally. Mass transport problems of free-breathing fuel cells were also studied. These cells rely on free convection to provide reactants and remove reaction products. In this thesis, the aim was to develop an accurate model that is also computationally light.

The compression distribution in a stack was modelled based on an existing stack design. The results showed poor internal pressure distribution, with most of the cell experiencing insufficient compression. The modelling was then used to find a better end plate structure and suitable torques for the nut and bolt assemblies. The results were validated experimentally.

The effect of compression was studied on a local scale on which compression variations caused by the channel structure had been seen to affect the gas diffusion layer properties and contact resistances between components. According to the modelling results, there are strong local transversal electric currents in the cell. This phenomenon can affect the cell performance and lifetime negatively.

Suvi Karvonen .Modelling approaches to mass transfer and compression effects in polymer electrolyte fuel cells [Polymeerielektrolyyttipolttokennojen massansiirron ja puristuspaineen vaikutusten mallintaminen]. Espoo 2011. VTT Publications 772. 73 s. + liitt. 66 s.

Avainsanat PEMFC, fuel cell, modelling

Tiivistelmä

Väitöskirja käsittelee polymeerielektrolyyttipolttokennon (PEMFC) toiminnan mallinnusta paikallisesti ja kennotasolla. Tutkimuksen työkaluna käytettiin mallinnusta elementtimenetelmään perustuvalla ohjelmistolla. Mallinnuksen painopisteinä olivat erityisesti aineensiirron ongelmat ja puristuspaineen jakautuminen ja vaikutus kennon paikalliseen toimintaan.

Aineensiirtoa eli virtauskanaviston toimintaa tarkasteltiin kennon katodilla mallintamalla kanavistoon syntyvää virtausprofiilia. Kanaviston geometriaa muuttamalla pystyttiin parantamaan virtausprofiilia, ja tämä mallinnuksen avulla suoritettu optimointi havaittiin myös kokeellisesti. Aineensiirron kysymyksiä tutkittiin myös vapaasti hengittävien polttokennojen kohdalla. Näissä kennoissa aineensiirto perustuu vapaaseen konvektioon. Työssä pyrittiin kehittämään yhtä aikaa luotettava ja laskennallisesti kevyt malli. Lopputuloksena syntyi kolmiulotteinen malli vapaasti hengittävästä kennosta, jolla tutkittiin kennon koon ja asennon vaikutusta toimintaan.

Kennostossa vallitsevaa puristuspainetta mallinnettiin olemassa olevaan kennostoon perustuvan mekaanisen mallin avulla. Tuloksena saatiin epätasainen painejakauma. Mallinnuksen avulla etsittiin parempi rakenne kennoston päätylevyille sekä muutettiin pulttien vääntömomentteja, jolloin kennolla vallitseva painejakauma saatiin pysymään toivotuissa rajoissa. Samalla päätylevyn painoa saatiin vähennettyä. Tulokset verifioitiin kokeellisesti.

Puristuspaineen vaikutusta tutkittiin paikallisella tasolla, jossa virtauskanaviston rakenteen aiheuttamien painevaihteluiden oli todettu vaikuttavan merkittävästi kaasudiffuusiokerrosten ominaisuuksiin ja komponenttien välisiin resistansseihin. Mallinnuksen tulosten mukaan kennossa syntyy paikallisesti merkittävästi poikittaissuuntaista sähkövirtaa, joka aiheuttaa virrantiheyteen vaihteluja. Ilmiö voi vaikuttaa negatiivisesti kennon toimintaan ja elinikään.

Preface

This thesis was written in the Applied Physics department of the Helsinki University of Technology, in the New Energy Sciences Group, supervised by Professor Peter Lund. However, at the time of publication, this university has ceased to exist and is now a part of Aalto University.

The majority of funding came from the National Technology Agency of Finland (Tekes), the Wihuri Foundation and the National Graduate School for Energy Technology, all of which I thank for their support.

I want to thank all the people I had the pleasure to work with, especially Tero Hottinen, Mikko Mikkola, Olli Himanen and Iwao Nitta. The work you did gave me the basis to build on. The fuel cell group had some great people in it, and I enjoyed working with all of you.

Thank you to my friends, for our teamwork throughout student times, for keeping me sane and in touch with other people during the baby year and for easing my return to work. You were surely the best support group ever.

My thanks to family: my husband, who put up with me not having a real job, so to say, for the years of making this thesis and never would have even thought to complain. My parents, who made sure I had everything I needed when it was time to choose what I wanted to do with my life. And finally, my son, who is the most important thing to come out of these years of my life. Maybe one day you will read this and know better than we now do what became of fuel cells.

Contents

List of Publications

1. **Modeling of flow field in polymer electrolyte membrane fuel cell**
   Karvonen, S., Hottinen, T., Saarinen, J., Himanen, O.
   Journal of Power Sources 161(2), pp. 876–884 (2006)

2. **Inhomogeneous compression of PEMFC gas diffusion layer. Part II. Modeling the effect**
   Hottinen, T., Himanen, O., Karvonen, S., Nitta, I.
   Journal of Power Sources 171(1), pp. 113–121 (2007)

3. **Modelling the effect of inhomogeneous compression of GDL on local transport phenomena in a PEM fuel cell**
   Nitta, I., Karvonen, S., Himanen, O., Mikkola, M.
   Fuel Cells 8(6), pp. 410–421 (2008)

4. **Modeling of polymer electrolyte membrane fuel stack end plates**
   Karvonen, S., Hottinen, T., Ihonen, J., Uusalo, H.
   Journal of Fuel Cell Science and Technology 5(4), art. no. 041009-1 (2008)

5. **Modeling free convective mass and heat transfer in fuel cells**
   Karvonen, S. Submitted to Journal of Fuel Cell Science and Technology (2011)

Author's Contributions

For Publication 1, the author was mainly responsible for building the model, conducting the experiments, analysing the data and writing the article.

For Publication 2, the author participated in the modelling and made a minor contribution to writing the article.

For Publication 3, the author participated in building the model, analysing the data and writing the article.

For Publication 4, the author was mainly responsible for designing and building the model and analysing the modelling data. The author participated in planning the experimental part and analysed the experimental results. The author was mainly responsible for writing the article.

For Publication 5, the author was mainly responsible for designing and building the model as well as analysing the data and writing the article.

List of Symbols

Symbol	Quantity	value/unit
A	area	m^2
c	concentration	mol/m^3
c_p	thermal capacity	J/kgK
D	binary diffusion coefficient	m^2/s
$\tilde{D}$	Maxwell–Stefan diffusion coefficient	m^2/s
E	energy	J
E_{theor}	theoretical fuel cell open circuit voltage	V
F	Faraday constant	96485 C/mol
$\mathbf{g}$	gravity vector	m/s^2
G	Gibbs' energy	J/mol
H	enthalpy	J/mol
$\mathbf{i}$	unit vector, x-direction	-
$\mathbf{J}$	molar flux vector	mol/m^2s
$\mathbf{j}$	unit vector, y-direction	-
j	current density	A/m^2
$\mathbf{k}$	unit vector, z-direction	-
k	heat conductivity	J/m^2
M	molar mass	kg/mol
$\mathbf{n}$	normal vector	-
$\dot{\mathbf{N}}$	molar flux on electrode boundary	kg/m^2s
p	pressure	Pa
R	gas constant	8.314 J/molK
S	source term	-
$S_{a,c}$	entropy at cathode or anode	J/K
T	temperature	K
$\mathbf{t}$	tangential vector	-
q	thermal flux	W/m^2
$\mathbf{u}$	velocity vector	m/s
u	x-directional velocity	m/s
V	volume	m^3

v	y-directional velocity	m/s
w	z-directional velocity	m/s
x	molar fraction	-
z	number of electrons involved in a reaction	-

Greek symbols

α	reaction symmetry factor	-
γ	strain (tensor)	-
Δ	change	-
ε	porosity	-
η	dynamic viscosity	Pa s
η_{theor}	theoretical efficiency	-
κ	permeability	m^2
σ	electrical/ionic conductivity	Sm^{-1}
σ_{str}	stress (tensor)	Pa
φ, Φ	potential	V
ρ	density	kg/m^3
ω	mass fraction	-

Subscripts and superscripts

0	reference state
A	reducing component
B	oxidizing component
ch	channel system
CL	catalyst layer
con	mass conservation equation
D	Darcy's Law
eff	effective
GDL	gas diffusion layer
H2	hydrogen
H2O	water
i	species
m	ionic potential
mass	mass-averaged formation of Maxwell–Stefan equations

mem	membrane
molar	molar-averaged formation of Maxwell–Stefan equations
NS	Navier–Stokes equation
O2	oxygen
ref	reference concentration
s	electronic potential
theor	theoretical

Acronyms

1D	one-dimensional
2D	two-dimensional
3D	three-dimensional
AFC	alkali fuel cell
BP	bipolar plate
BMW	Bayerische Motoren Werke AG
CHP	combined heat and power production
DMFC	direct methanol fuel cell
FC	fuel cell
FEM	finite element method
GDL	gas diffusion layer
GE	General Electric
MCFC	molten carbonate fuel cell
NASA	National Aeronautics and Space Administration
PAFC	phosphoric acid fuel cell
PEMFC	polymer electrolyte membrane fuel cell
PEM	polymer electrolyte membrane
PFSA	perfluorosulfonic acid
SOFC	solid oxide fuel cell

1. Introduction

Energy production often has a negative impact on the environment. In historical times, small populations and the nature of the available energy sources ensured that energy production was sustainable or, at least, that any harmful effects such as deforestation were local, not global. However, with the rapidly increasing global population and improving standard of living, the problem of providing clean energy for everyone has become one of the main challenges of the 21st century. Currently, there does not appear to be any single solution that can be used universally to produce clean, inexpensive energy. Instead, we face multiple choices that all have their advantages and disadvantages.

One proposed solution to the problem of environmentally sustainable energy production is the so-called hydrogen economy in which one of the main energy carriers is hydrogen (as opposed to, e.g., oil and electricity). Hydrogen can be produced by various methods and used in, for example, fuel cells. The use of hydrogen production processes, which do not produce greenhouse gases, would, in theory, allow the hydrogen economy to function with a minimal negative effect on the climate. Moving to a hydrogen economy would be expensive, however, and require much political will and time. Several technical issues concerning hydrogen production, storage, delivery and use in fuel cells would also need to be solved before a hydrogen economy could be considered a realistic alternative. As a consequence of these difficulties, the hydrogen economy is currently a relatively utopian scenario that may never be realized. Hydrogen and fuel cells could be part of the solution, however, even if the road of the hydrogen economy is never taken.

A fuel cell is a device that produces electrical and thermal energy from various fuels such as hydrogen, methanol or natural gas. A fuel cell can convert the chemical energy of its fuel and oxidant into electricity without combustion or conversion through thermal energy, which, at least in theory, gives it high effi-

ciency. If hydrogen is used as the fuel, the only reaction product is water, so there are no harmful exhaust compounds, at least not on site. Fuel cells also have high power density, are silent, require little maintenance and, on a small power scale, usually have high efficiencies compared with many traditional technologies such as the internal combustion engine.

Different types of fuel cells are suitable for applications ranging from milliwatts to megawatts and from portable to stationary. The different types of fuel cells are usually categorized by their operating temperature or materials. Fuel cells can potentially be used in everything from portable electronics and automobiles to small-scale power plants. The fuel cell type of interest in this thesis is the polymer electrolyte membrane fuel cell (PEMFC), which is best suited to portable electronics, transportation and other small-scale applications.

Unlike internal combustion engines, fuel cells retain their good efficiency at partial loads. However, for each application, fuel cells must first be proven superior to existing technologies such as batteries, internal combustion engines and the electrical network. Fuel production, storage and distribution issues also have to be solved. Currently, fuel cell performance, life-time and price are not viable for anything but small niche applications, and wide-scale commercialization is yet to come.

In principle, fuel cell performance can be improved either by using new, superior materials and innovations or by improving the cell design and operational conditions. In the case of PEMFC materials, the research includes finding new electrolyte membranes that can operate at a higher temperature without the need for liquid water, researching catalysts in order to decrease price and increase efficiency and lifetime, improving gas diffusion layer properties and finding more corrosion-resistant materials for the support structures. Cell design can be improved by, for example, optimizing flow field geometry, improving the compression distribution in a stack or finding new, innovative solutions. Finding the optimal operating conditions, i.e., the temperature, current, gas flow stoichiometry, etc., is also crucial to cell performance.

The subject of this thesis consists of finding ways to improve the performance of the PEM fuel cell through modelling. Many fuel cell phenomena are difficult or almost impossible to experiment on and cannot be deduced from the overall cell performance. In these cases, modelling is an invaluable tool. Modelling can also speed up the process of improving cell design, as simulation is often less expensive and less time-consuming than experimentation. In this thesis, modelling is used for studying cell phenomena and for improving cell design. The

results provide new insight into local phenomena and demonstrate that certain changes in design parameters can improve cell performance significantly.

The distribution of reactants on a fuel cell cathode is studied in Publication 1 and discussed in Chapter 4. This study focused on the geometrical design of the flow field plate structure and demonstrated that small changes in geometry can improve flow distribution significantly, i.e., make it more even in the cell. This is important in terms of overall cell performance, as an uneven flow distribution will cause problems such as reactant starvation and accumulation of liquid water in the cell. Modelling is a natural way to approach a problem for which in-situ experiments, though possible, are complicated and time-consuming. The modelling results obtained in Publication 1 were verified experimentally and are in agreement on a qualitative level.

Publications 2 and 3 focus on the local phenomena caused by uneven compression in the cell. A fuel cell is usually compressed by a nut and bolt assembly so that the cell does not leak gases and the components have good electrical contact. The pressure deforms the soft gas diffusion layers used in fuel cells, however, crushing their pores, and excessive compression thus leads to mass transport problems. Furthermore, the internal structure of a PEMFC, i.e., the channel system of the bipolar plates, leads to large local variations in compression pressure as there is practically no compression on the gas diffusion layers underneath the channels. This causes large variations in many key parameters such as the electronic conductivity, the mass transport properties of the gas diffusion layers and the contact resistance between different components. This phenomenon has been largely neglected in previous studies.

A basic model for studying the effects of uneven compression was developed in Publication 2. The results showed that local effects are significant, especially in terms of current density. Some of the parameters used were inaccurate however. These parameters were studied experimentally in order to improve the reliability of the model. The new improved model was reported in Publication 3. The results show that due to uneven compression and thus varying contact resistances and uneven deformation of the gas diffusion layer, the current density in the electrodes has a large transversal component and a local maximum. In earlier modelling studies, the compression effects were excluded and the current was mostly seen to travel straight from the electrodes to the current collectors. The local variations discovered here are significant as they can have a negative effect on the overall performance as well as the lifetime of the cell.

Publication 4 focuses on studying the compression in the cells on a larger scale. The pressure distribution in a stack was studied by making a mechanical model of an existing PEMFC stack. The results showed that the pressure on the gas diffusion layers of the individual cells was far from in the optimal range. The model was then used to find an improved end plate structure that was both lighter and more rigid than the original in order to improve the internal pressure distribution. The torque on the nut and bolt assemblies was also optimized. As a result of these changes, it was possible to limit the internal pressure in the cell to an optimal range. The modelling results were validated experimentally on a qualitative level.

Publication 5 focuses on the mass transfer of a free-breathing fuel cell, i.e., a fuel cell that relies on natural convection instead of auxiliary equipment such as pumps to take care of its mass transport. The model built in this study focused on the cathode and its surrounding air zone. 2D and 3D models were used to find the best way to model the problem accurately and with computational efficiency. The resulting model was then used to study the performance of a small, free breathing fuel cell. The results show, e.g., that the tilt angle of the cell has a large impact on the performance.

The subjects of these studies thus cover cell and local-scale phenomena, mass transport issues and compression effects. The uniting factor is the aim to gain a better understanding of the way PEMFC operates beyond a few variables like current and voltage, which are easily measured externally but do not say much about the complex phenomena occurring internally. The modelling has much room for improvement in future work, as PEMFC operation is based on many different, interdependent and complicated phenomena for which the correct parameters and correlations are often not well known. Nevertheless, the modelling in this study has offered new scientific information on various cell phenomena, and the models can be used as tools to optimize cell performance.

2. Fuel Cells

2.1 History

Fuel cells are often thought of as modern technology that is not yet ready for commercialization. The concept of the fuel cell dates back to 1838–1839 when Christian Schönbein published the principle of the fuel cell [1]. In 1845, the first functional fuel cell was built by Sir William Grove [2]. At the time, not much practical value was attached to this phenomenon and fuel cell development did not advance for decades.

The term “fuel cell” was first proposed by Ludwig Mond and Charles Langer, who built a fuel cell operating on air and industrial coal gas in 1889 [3]. After Mond and Langer, no significant advancement was made before the 1950s, when Francis T. Bacon and his group replaced the previously used platinum electrodes and acid bath electrolyte with less expensive nickel electrodes and alkaline electrolyte. After almost twenty years of research, Bacon developed a five kilowatt fuel cell [4]. In the 1950s, fuel cells were also being developed at the General Electric (GE) Company. The results achieved by Bacon and GE showed that fuel cells, although expensive, were not limited to the laboratory but had potential for real applications. GE was also the company that built the first polymer electrolyte membrane fuel cells in the 1960s [5]. Not surprisingly, the first instance of adoption of the new technology was by the National Aeronautics and Space Administration (NASA), whose spacecraft required a source of electricity [6]. Nuclear power was considered too hazardous while a combination of solar power and batteries would have been too bulky. As a consequence, fuel cells were used in the Gemini, Apollo and Space Shuttle missions. During this time, fuel cells were considered for many different applications, an example of which is the Allis-Chalmers fuel cell tractor in Figure 1.

Figure 1. An experimental Allis-Chalmers fuel cell tractor in 1959 [7].

For the past few decades, increasing awareness of the limited fossil fuel resources and the environmental effects of their use have given ample motivation for research into new energy technologies, one of which is fuel cell technology. Consequently, during the last twenty years, fuel cell research has boomed. This is partly due to the development of new materials that were not available earlier, such as improved electrode materials.

Traditionally, the greatest interest in fuel cell technology has perhaps come from the automotive industry, though fuel cells can also be used in portable electronics and for stationary power production. In transportation, the first demonstration fuel cell bus was built by Ballard in 1993, after which demonstration fuel cell buses have been in use in many cities. Demonstration fuel cell cars by companies such as Ford, Toyota and BMW have been presented since the late 1990s. Demonstration projects are still going on, and a fuel cell bus fleet of 20 buses was operational during and after the 2010 Winter Olympics [8].

On a smaller scale, fuel cells can be used in portable applications such as laptops and cell phones. These devices require increasing amounts of power, and providing this for long periods is challenging with current battery technologies. The operating conditions in these applications vary greatly, as does the size of the fuel cell system, and the auxiliary equipment, in particular, has to be minimized. One candidate for these systems is a so-called free-breathing fuel cell that takes its oxygen from the surrounding air through passive mechanisms.

Current fuel cell research aims to lower the cost and improve the performance and lifetime of the cells, thus making fuel cells a viable alternative to competing technologies. The European Union has a programme called the Fuel Cells and Hydrogen Joint Technology Initiative. The strategic research agenda, written in 2005, cites 4000 €/kW as the current price and 100 €/kW as the goal price for FC systems in transportation [9].

2.2 Basics of Fuel Cells

A fuel cell is an electrochemical apparatus that uses the chemical energy of its fuel and oxidant. There is no combustion in the process. The advantage over internal combustion engines is that the efficiency of the fuel cell is not bound by Carnot efficiency. This conversion is accomplished by separating the fuel and oxidant by an electrically insulating but ionically conductive electrolyte. Fuel is fed to the anode and oxidant to the cathode. The fuel, driven by the chemical potential, is oxidized on the anode, while the oxidant is reduced on the cathode. The resulting ions pass through the electrolyte from the cathode to the anode or vice versa depending on the fuel cell type. The electrons travel via an external circuit, thus producing electric current that can be used as desired.

Fuel cells are typically categorized according to the electrolyte material, though some cell types are named after their fuel. In general, fuel cells can be divided into two main categories: high or intermediate temperature cells, such as the Solid Oxide Fuel Cell (SOFC), and low temperature cells, such as the Polymer Electrolyte Membrane Fuel Cell (PEMFC). Potential fuels include, e.g., hydrogen, methanol and methane, and the range of suitable fuels depends on the cell type. In general, high temperature fuel cells can use a wider range of fuels, especially hydrocarbons, than low temperature fuel cells. The oxidant is oxygen, either as a pure gas or obtained from the air. The basic structure of the cell is independent of the cell type and consists of two electrodes separated by an electrolyte layer. The most common electrolyte materials are polymer membranes with sulfonic acid groups, ceramic materials, acids and molten salts. The most common fuel cell types and their characteristics are listed in Table 1.

High temperature cells are suitable for stationary power production and operate at 700–900 °C. Intermediate temperature SOFCs that operate at 500–700 °C are also being researched. Low temperature FCs such as PEMFCs operate in the temperature range of liquid water and can be employed in a variety of applications from portable electronics to transportation, small-scale residential heat and

power production and many niche applications [2]. In recent years, the lines have become blurred, however, as low temperature SOFCs (500–700 °C) and high temperature PEMFCs (over 100 °C) have been researched. The ultimate goal of fuel cell technology, the fuel cell car, would probably employ a PEMFC, although there has also been research into SOFCs.

Table 1. Fuel cell types, their operating temperatures and electrolyte materials.

Fuel cell type	**Abbreviation**	**Operating temperature**	**Electrolyte material**
Polymer Electrolyte Membrane	PEMFC	20–90 °C	Proton-conducting polymer film
Direct Methanol	DMFC	20–90 °C	Proton-conducting polymer film
Alkaline	AFC	100–250 °C	OH^--conducting alkaline solution
Phosphoric Acid	PAFC	200 °C	Proton-conducting phosphoric acid
Solid Oxide	SOFC	700–1100 °C	O^{2-}-conducting ceramic oxide[1]
Molten carbonate	MCFC	600–700 °C	CO_3^{2-}-conducting molten carbonate

For portable applications, the main competition is batteries, whose efficiency is very high and price low. Despite rapid improvement, the energy storage capacity of batteries is not sufficiently high for many applications. Laptops, in particular, are seen as a potential application for fuel cells, as their batteries can currently only provide energy for a few hours of use, and the power consumption of these devices is continually increasing. With fuel cells, this period could perhaps be extended as the energy capacity would depend only on the size of the fuel supply not the cells themselves. In a fuel cell, the power and energy capacities can be sized separately whereas in batteries they are interdependent. A fuel cell laptop does not require recharging, though it does need refuelling. If it is necessary to use a laptop for a long period with no external source of electricity, it is easy to have several fuel containers ready.

In transportation, the competing technologies are the traditional internal combustion engine running on ever-decreasing reservoirs of fossil fuels (or biofuels) and the yet to be commercialized electric car running on batteries. Fuel cells

[1] There are also some ceramic materials that exhibit proton conductivity, see, e.g. [10].

would be ideal for transportation applications, but the necessary fuel distribution infrastructure does not yet exist. The operating conditions are also harsh on the cells, for instance, the ambient temperature can be as low as -30 °C. In a true hydrogen economy, fuel cells could also be used to produce combined heat and power (CHP) for distributed energy production. On a smaller scale, fuel cells could be used to produce CHP from natural gas at the end of a gas line, or using landfill gas or biogas.

Currently, fuel cells are mostly used for demonstrations and military applications. There are some niche applications for which fuel cells could be used in the near future however. These include telecommunications link stations and other off-grid applications. Ships and boats may benefit from a fuel cell system that produces electricity while the engines are off and the battery capacity is insufficient.

2.3 Polymer Electrolyte Membrane Fuel Cell

The PEMFC is a low temperature fuel cell that has a solid polymer membrane with sulfonic acid groups as an electrolyte. The PEM fuel cell uses hydrogen as fuel and oxygen (typically in the air) as the oxidant. The electrode and cell reactions are:

Anode: $H_2 \rightarrow 2H^+ + 2e^-$ (1)

Cathode: $\frac{1}{2}O_2 + 2H^+ \rightarrow H_2O$ (2)

Full cell: $H_2 + \frac{1}{2}O_2 \rightarrow H_2O$ (3)

Thus, in a PEMFC fuel cell, the only reaction product is water. Combined with its other attributes, low operating temperature, fast start-up and shutdown, high efficiency and the possibility of scaling the stack according to power requirements, the PEMFC is suitable for a wide range of applications.

The heart of each PEMFC is composed of the electrolyte, electrodes, gas diffusion layers and flow field plate. In a stack, i.e., multiple cells connected in series, the flow field plates of adjacent cells are typically combined and the result is known as a bipolar plate. The electrodes are usually coated on a polymer electrolyte film. This structure is known as the membrane electrode assembly (MEA). As a single cell usually gives a voltage of less than 1 V, it is usual to connect many cells in series to form a fuel cell stack. In addition to the cells themselves, stacks usually have components known as end plates, which provide

mechanical support for the cells. These components are described briefly in the following sections. It should be noted that in addition to these components, a fuel cell system also requires support structures such as gaskets, nuts and bolts, fuel and exhaust lines, flow controllers, electrical components, etc.

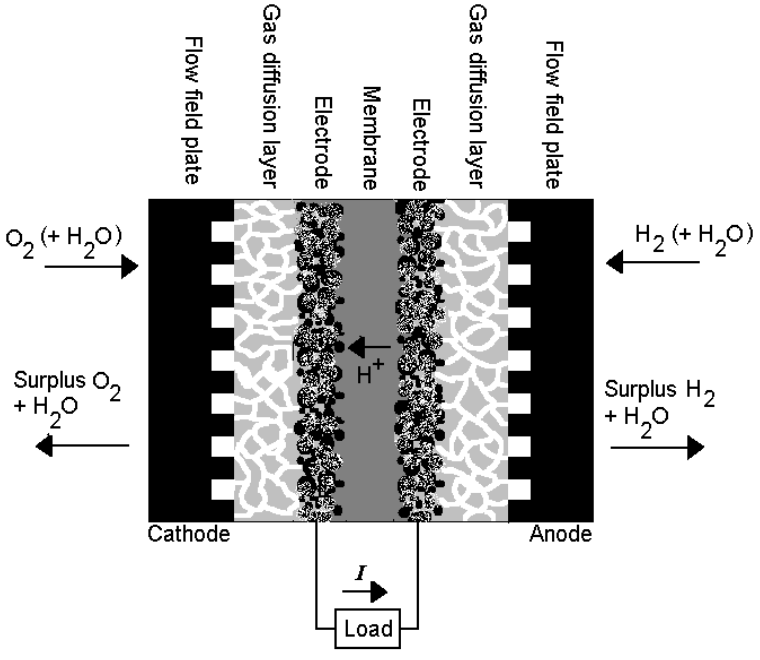

Figure 2. A schematic of a PEMFC. Picture is not to scale.

2.3.1 Membrane Electrode Assembly (MEA)

The most commonly used electrolyte of the PEMFCs is the Nafion® membrane, a solid ion-conducting perfluorosulfonic acid (PFSA) material. It consists of sulfonic acid groups attached to a polymer matrix, the former providing proton conduction and the latter structural support. There are many ion transport mechanisms through which the membrane conducts protons from the anode to the cathode and they are all dependent on the presence of water molecules in the membrane. Thus, a dry membrane does not conduct ions. The membrane drying out not only lowers the fuel cell performance but can also lead to actual membrane damage and thus to shorter lifetimes. The requirement for liquid water also limits the temperature range of the cell.

The electrodes are composed of carbon black, ion-conducting polymer and catalyst particles. The use of catalysts, usually platinum, is necessary in all low temperature cells, as the reaction kinetics in this temperature range are too slow to achieve good enough cell performance otherwise. The electrode is porous in order to maximize the amount of active surface area. Porosity is also required in order to provide transportation for the reactants and reaction products. The catalyst particles are very sensitive to many impurities in the air or fuel, especially sulphur and carbon monoxide, and usually degrade or agglomerate even in normal operation, thus lowering the cell lifetime.

The dependence on the presence of liquid water everywhere in the membrane is a challenge for mass transportation, as excess water tends to block oxygen transport to the reaction sites, thus reducing the cell reactions. This phenomenon is known as flooding. There is thus a fine balance between too much and too little water in the cell. Water management is one of the most important and challenging aspects of PEMFC operation. It has been studied by many groups, and a good review on this subject was published in, e.g., [11].

The lifetime and durability of the MEA have been studied by many groups, as MEAs have been observed to degrade relatively quickly. There are several mechanisms of MEA degradation, e.g., membrane thinning or cracking, contamination, electrode layer delamination and catalyst particle agglomeration, dissolution and migration as well as chemical reactions of the catalyst particles, see, e.g., [12–17]. These mechanisms may be enhanced by inadequate temperature or water management, impurities, severe operating conditions and voltage cycling, see, e.g., [18, 19]. Thus, it is crucial that the cell operating parameters and structures are designed so that these issues can be avoided as far as possible. Compression, flow and temperature distributions across the cell are not only important to the performance of the cell but also to its lifetime. Thus, the modelling of these issues, such as described later in this work, also has ramifications in terms of MEA durability and consequently cell lifetime.

2.3.2 Gas Diffusion Layers

Gas diffusion layers (GDLs) provide transportation for reactants and reaction products between the flow channels and MEA. They are also electrically conductive, provide mechanical support for the fragile MEA and have to be chemically inert in the fuel cell environment. GDLs have conflicting requirements for optimal performance: they have to be porous to allow for mass transport while at

the same time being mechanically durable and good electrical conductors. These properties also depend on the compression, as the soft porous material is deformed under mechanical stress. When a fuel cell is assembled, the GDL is compressed under the flow field plate ribs while the part under the channel remains almost uncompressed, leading to significant local variations in porosity and electrical conductivity.

GDLs also have to be able to transport water, i.e., the liquid water required in the MEA and created in the cathode reaction. GDLs are typically made of carbon paper or cloth, with a hydrophobic component such as polytetrafluoroethylene (PTFE, commonly known as Teflon®). It is also usual to add a so-called microporous layer of PTFE and carbon black on the electrode side of the GDL in order to improve its water transport properties, see, e.g., [20, 21].

2.3.3 Bipolar Plates

Bipolar plates envelop the GDLs and MEA. They are typically much thicker and mechanically more rigid than the thin GDL and MEA layers and thus constitute the mechanical support for the cell. Bipolar plates are good electrical conductors and are part of the route electrons travel on their way to the external circuit. They also have to be impermeable to gas. Bipolar plates are traditionally made of metal, typically stainless steel, or graphite. Of these, graphite has been widely used in laboratory experiments but is unsuitable for wide-scale commercialization because it is expensive and hard to machine or shape. Metal plates would otherwise be ideal due to their high conductivity, ready availability and ease of manufacturing, but in the corrosive fuel cell environment they do not remain chemically inert and the resulting dissolved particles can damage the MEA. Thus, alternative materials such as polymer composites, see, e.g., [22, 23], which will not corrode in the fuel cell environment and have the added advantage of being lighter than metal, have been studied by many groups. An alternative solution is to coat the metal with a thin corrosion-protective layer, see, e.g., [24–26].

Bipolar plates should have good electrical contact with the GDLs while also being able to transport the reactants and reaction products to and from the GDL. In order to accomplish this, the plates have channels grooved on their faces to direct the mass flows in the desired directions. The design of the channel system or flow field governs how the reactants are distributed on the GDLs and thus on the electrode surfaces, as well as affecting the removal of excess water from the cell.

As the channels may be set in any geometrical arrangement imaginable, there are various possible flow field configurations. It is also possible to fill the channels with porous media, partially or completely, in order to improve flow distribution and liquid water management, see, e.g., [27, 28]. Four different types or a combination of them are usually used in fuel cells: the parallel, serpentine, interdigitated and spiral flow fields, see, e.g., [29–31]. The width, depth and cross-sectional shape of the channels as well as the distance between two channels (a.k.a. land or rib width) are all adjustable and have a significant effect on the cell performance, see, e.g., [32–34]. Serpentine and spiral flow fields have long channels, which usually give a relatively even reactant distribution but cause a larger pressure drop thus requiring more from auxiliary equipment (pumps). The interdigitated flow field has short, discontinuous channels, which force the reactant flow into the GDL and cause a large pressure drop. Of these four alternative configurations, the parallel flow field is the only one that does not cause a large pressure drop across the cell. If, however, the flow field design is not planned with care, the resulting flow distribution can be very uneven. This has caused many to dismiss the parallel flow field. An uneven flow distribution causes reactant starvation on some parts of the electrode, which decreases the overall performance of the cell. The flow distribution in a parallel flow field system and its optimization was studied in this thesis and is discussed in Chapter 4 and Publication 1.

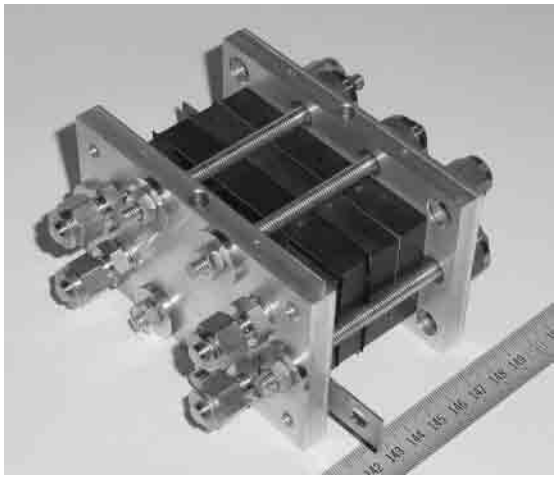

Figure 3. A small PEMFC stack used in the Laboratory of Advanced Energy Systems in ca. 2001 (Photo courtesy of Mikko Mikkola).

2.4 Free-Breathing Fuel Cells

It is possible to build a fuel cell that takes its required oxygen from ambient air without auxiliary equipment. This kind of fuel cell is known as a free-breathing fuel cell. It relies on the temperature difference between the cell and ambient air created by the heat produced in the cell operation to drive oxygen to the cell by natural convection. Free-breathing fuel cells are typically suited to small-scale applications requiring little power such as transportable electronics. They need less auxiliary equipment than fuel cells, depending on forced convection and so require less space and cost less.

The performance of a free-breathing fuel cell depends on the natural convection, which, in turn, is affected by the geometrical design, size and orientation of the fuel cell. The cathode usually requires a cover structure to avoid mechanical damage, the design of which is also important in terms of natural convection. The effectiveness of natural convection on the cathode of a free-breathing fuel cell has been studied in Publication 5 and is discussed in Chapter 7. The aim was to develop a model capable of describing this phenomenon and giving predictions on how the size and position of the cell affect its performance.

2.5 PEMFC Performance

The theoretical open circuit voltage E_{theor} of a PEMFC is calculated from the Gibbs energy ΔG of the chemical reaction of hydrogen and oxygen combining to produce water [2]:

$$E_{theor} = -\frac{\Delta G}{zF} \tag{4}$$

Here, z is the number of electrons that participate in the reaction, two in the case of the PEMFC. F is the Faraday constant that gives the magnitude of the electric charge per mole of electrons, approximately 96,485 C/mol. At 25 °C ΔG is -237.2 kJ/mol and the open circuit voltage of the cell is 1.23 V.

The open circuit voltage depends on the temperature of the cell as well as the partial pressures of the reactants. This correlation is given by the Nernst equation:

$$E = E_{theor} + \frac{RT}{zF} \ln\left(\frac{p_{H_2} p_{O_2}^{1/2}}{p_{H_2O}} \right) \tag{5}$$

Here, E is the open circuit voltage, R the universal gas constant, T the temperature and p_i the partial pressure of species i.

The theoretical maximum efficiency of a fuel cell can be calculated from

$$\eta_{theor} = \frac{\Delta G}{\Delta H} \tag{6}$$

where ΔH is the enthalpy of the cell reaction. At 25 °C ΔH = -285.84 kJ/mol. Thus, the theoretical maximum efficiency of a PEMFC is 83%. This efficiency is, of course, never reached as other factors such as the degree of fuel utilization and internal resistances affect the efficiency. However, the efficiency of a PEM fuel cell is usually in the range 30–60% [2].

In reality, due to impurities and hydrogen cross-over causing mixed potentials, the open circuit voltage is usually slightly lower than E, see, e.g., [35]. In an operating fuel cell, the voltage is lower still, as drawing current from the cell causes overpotentials to occur. There are three main loss mechanisms present in an operating fuel cell: the activation overpotential, ohmic losses and the diffusion overpotential. These loss mechanisms are discussed briefly in the following paragraphs.

The activation overpotential is determined by the cell reaction kinetics, especially the slow cathode reaction. The activation overpotential is typically the largest loss factor. It can be somewhat mitigated by using catalysts and raising the cell temperature. The activation overpotential is almost solely responsible for performance losses in low current densities.

Ohmic losses are caused by the resistance of the cell materials and contact resistances between the components to ionic (membrane) and electric (GDL, flow field plates, etc.) currents. The magnitude of ohmic losses is directly proportional to the amount of current drawn from the cell. Ohmic losses can be reduced by improving the electrical conductivity of the cell materials, especially the membrane, and ensuring good electrical contact between the cell components (especially the electrodes and the GDL, and the GLD and the flow field plates). The former depends on the materials used and the humidity of the membrane, while the latter also correlates to the compression directed at the cell or stack (discussed in more detail in Chapter 5). Ohmic losses determine the shape of the current-voltage curve in middle current densities.

The diffusion overpotential is caused by the mass transportation limitations. As an increasing amount of current is drawn from the cell, the reactant concentration becomes low at the electrodes and the reaction product water starts to

block the reaction sites. Thus, the diffusion overpotential is large at high current densities. It can be reduced by employing more powerful pumps, optimizing the channel system in the flow field plates and improving mass transfer in the GDLs (e.g., by making them more porous or hydrophobic).

In addition to these mechanisms, performance losses may be caused by impurities in the cell, either mixed in the air or fuel, or dissolved from the cell components; hydrogen leaking through the membrane in molecular form to the cathode, etc. When all these mechanisms are taken into account, the voltage of an operating fuel cell is typically around 0.6–0.7 V. Connecting multiple cells in series gives more practical voltages. It is of course possible to operate the cell at any voltage between the open circuit voltage and zero, but this does not usually give optimal power or efficiency.

The current density j of the cell and the overpotential φ correlate according to the following equation [2]:

$$j = j_0 \frac{c_A}{c_{A,ref}} \exp\left(-\frac{\alpha z F \varphi}{RT}\right) - j_0 \frac{c_B}{c_{B,ref}} \exp\left(\frac{(1-\alpha) z F \varphi}{RT}\right) \tag{7}$$

This equation applies to both electrodes. Here, j is the current density, φ the overpotential, c_A and $c_{A,ref}$ the concentration and reference concentration of the reducing component and c_B and $c_{B,ref}$ of the oxidating component. j_0 is the so-called exchange current density that represents the current at the open circuit voltage when no net current is drawn from the cell, and α is the reaction symmetry factor. A simplified form of this equation is known as the Butler-Volmer equation, and the name is often mistakenly applied when this equation is used.

3. PEMFC Modelling

A fundamental approach to developing any technology is to conduct experiments. Experimentation has some limitations, however, that often make studying a given aspect very difficult or even impossible. For example, local phenomena, i.e., small-scale differences in current density, are almost impossible to measure in any way but are important in terms of overall efficiency and cell lifetime. In general, it is easy to measure an IV-curve of a cell; it is much harder to ascertain which factors determined the shape of that curve and how. Modelling can also be used to investigate the effect of a wide range of parameter values, while experimentation is often limited to a few values at a time. In many cases, modelling can be an invaluable tool, but the results of and the assumptions made during the modelling must always be reviewed critically, and experimental validation should be done whenever possible.

PEMFC modelling is typically based on modelling one or more of the following phenomena:

- mass transfer, i.e., modelling fluid, species and two-phase behaviour of water
- heat transfer
- charge transfer
- electrochemistry of the cell reactions
- mechanical stress, i.e., internal compression pressure.

Although the principle is fairly simple – hydrogen and oxygen react to form water, heat and electricity – the modelling of the cell phenomena is quite complicated. The different length scales involved are one reason for this complexity as fuel cell phenomena. In short, the fuel cell phenomena occur in:

- the nanometre range, modelled by density-functional theory and molecular dynamics
- the micrometre range or the material structure level
- the millimetre – metre scale for flow dynamics, mass, heat and charge transfer by continuum mechanics.

The time scales are as diverse, as electrochemical phenomena occur very quickly, whereas the mass and heat transport phenomena are slower[2]. These different time and length scales cannot be handled by a single model; instead each model usually focuses on one of these.

It is practically impossible to create a fuel cell model that takes into account all of the complex phenomena occurring in the cell. In a sense, this is true of all modelling beyond a few simple systems – the underlying physics of quantum mechanics cannot be used in its exact formulation for modelling on a macroscopic level. Even when considering classical physics, however, the various phenomena occurring in a fuel cell translate into a complex, nonlinear differential equation system. In addition to the list in the previous paragraph, the contact pressure distribution, thermal expansion of the cell, and other mechanical stresses also affect cell performance. A full model should include a time dimension in order to account for changes in operating conditions and current drawn from the cell, even the degradation of the cell should be accounted for. Solving this system in three dimensions, under dynamic conditions and handling the different length scales, ranging from nanosized catalyst particles to a macroscopic stack structure, is not possible even with modern computers.

Thus, by necessity, any fuel cell model focuses on studying a few effects in certain simplified conditions. Typical examples are modelling the electrochemistry of the cell and studying mass transport with different flow field configurations. Early models were 1D or even 0D and often studied only parts of the cell (the cathode electrode and GDL, for example), but as computers have developed, 3D models have become common and it is possible to model the whole cell geometry, see, e.g., [32]. It is still necessary, to make many assumptions and simplifications to obtain a solvable model however. For example, the anode mass transfer is often excluded in modelling, as the performance limitations

[2] A more in-depth discussion on the time and length scales can be found in [36]. The focus of this study is SOFCs, but the same principles apply to modelling PEMFCs.

(slow reaction kinetics, flooding) are usually derived from the cathode. A brief review of fuel cell modelling can be found in Section 3.1.

Another complication is that some parameter values are chosen almost arbitrarily in the absence of experimental data or theoretically derived values. For example, the exchange current density in Eq. (D) is a necessary parameter in the electrochemical equations that form the basis of a fuel cell model. This parameter depends on various factors such as the amount of catalyst on the electrodes and the cell temperature. As a result, it is different for each fuel cell and very difficult to measure. It is very common simply to use parameter fitting so that the model outcome looks reasonable and is physically sensible. The values used for the exchange of current density between different publications can differ by as much as a factor of 10^4, see, e.g., [37], for a good comparison of values used in various studies. Thus, the results may seem correct but can be unreliable. Mistakes in the modelling (simple numerical errors or more profound problems) could have been concealed by choosing parameters so that good-looking results are obtained. Thus, there is no guarantee that predictions given for other parameters will correspond to reality, i.e., the results cannot be extrapolated.

The exchange of current density is only one example; many other problematic parameters exist, for example, in two-phase modelling (condensation and evaporation rates, capillary pressure equations). Most of the two-phase parameters used are derived from experiments on sand or soil, which makes using these correlations for the fibrous, partially hydrophobic GDL media questionable (see, e.g., [38]). It is usually also necessary to average many material properties that in reality are not isotropic, such as GDL porosity or the contact resistances between different layers in the cell, in the absence of more detailed data. The results obtained from these models may be accurate in terms of the whole cell but, at worst, grossly inaccurate at describing local phenomena.

All these difficulties do not rule out the fact that modelling is very useful when used correctly however. It is simply one of several tools and has its limitations just like everything else. Modelling results should simply never be taken at face value but approached critically. It should also be remembered that even though a given model may oversimplify or exclude one aspect of the fuel cell phenomena it may still give valuable data on other aspects. Models can be developed further as more experimental data on various parameters become available.

3.1 A Short Review of PEMFC Models

This section provides a brief review of how fuel cell modelling has evolved from the first 0D analytic models to the complex 3D models used today. The modelling studies discussed in this section have been divided according to the method, dimension and aim of the modelling. It is not easy to categorize fuel cell models, and many models do not fit into any of the categories discussed here, e.g., spherical agglomerate modelling, see, e.g., [39]. The following sections are intended to give the reader a general idea of FC modelling without going into detail, as it is not possible to include the whole spectrum of FC modelling within the scope of this thesis. More detailed reviews on FC modelling can be found in, e.g., [40, 41].

Analytical models

Fuel cell models typically use some computational tool such as the Finite Element Method (FEM). There are also models based on equations that are solved analytically. An analytical fuel cell model is always highly simplified and idealized. Typical simplifications include assuming a constant temperature and reactant concentration. The dimensions in which the model is solved are reduced to zero or one. The underlying physics is usually also simplified by linearizing equations that could not otherwise be solved analytically. The results are not very accurate, especially at larger current densities. Analytical models can be used to gain approximate current-voltage dependencies and performing short calculations on simple systems, see, e.g., [42, 43]. Analytical models give a basic view on the cell operation in ideal conditions. Although many early models were analytical, and numerical 3D modelling is now more common due to more powerful computers, analytical or semi-analytical modelling is still being performed, for example, in [44, 45].

Semi-empirical modelling

In many cases, the physics of the fuel cell phenomena is either not well understood or are difficult to incorporate into modelling for practical reasons. In order to solve or avoid these issues, researchers may resort to using empirically obtained differential or algebraic equations instead of more accurate, theoretically derived ones. Many fuel cell models employ some empirical correlations; a typical example is equations for calculating the conductivity of a partially humidified membrane. A widely used correlation for this parameter was suggested by

Springer et al. in [46]. Semi-empirical modelling is fairly common, examples of empirical cell models can be found in, e.g., [47–49]. Semi-empirical models are also used in stack modelling in which more detailed models would require too much computing capacity.

The use of semi-empirical relations is often necessary due to a lack of better alternatives, but it should be avoided when possible. Firstly, semi-empirical correlations usually apply to a certain parameter range outside of which they can be inaccurate. Failure to recognize this may lead to erroneous conclusions. Secondly, the use of empirical correlations does not further the cause of understanding the underlying physics of a fuel cell. Resorting to empirical correlations may prevent us from learning new mechanisms that could be manipulated in order to improve fuel cell performance. Semi-empirical models may be fairly accurate in modelling designs and materials that are already in use, but they cannot give predictions on how new, alternative materials or new innovative design could affect cell operation.

One-dimensional models

1D models can be analytical, but if the equations are not linearized they are usually solved by discretization and numerical algorithms. This has the benefit of making the results slightly more reliable. However, 1D models are still limited to the overall correlations for current and voltage and other fuel cell characteristics. The study of many local phenomena is beyond 1D models, which assume that the cell is identical in each direction and thus cannot take into account the difference between flow field plate ribs or channels. The early fuel cell models such as presented in [50, 51] were typically 1D with many simplifying assumptions. They focused on mass transport, water management and cathode flooding.

Two-dimensional cell models

2D models are typically either channel models or channel cross-section models. The former can be used to study how the reactant and reaction product concentrations vary along the channel as the reactants are consumed. The latter gives information on, e.g., how electrical current is conducted to the flow field plates. All 2D models share the assumption of an infinite planar cell. Flow fields and other 3D phenomena cannot be studied with 2D models. A typical 2D model consists of the MEA and GDLs, and symmetry boundaries are employed. According to the aim of the study, some cell components can be excluded, for in-

stance, if the aim is to study cathode mass transport, the anode side and even the membrane may be excluded. 2D models can be very useful in cases in which the computational power is not sufficient for making a 3D model. This is often the case if small geometrical details such as the thin electrode layers are included as a modelling domain. In such cases, the computational grid or mesh will be very fine, making the model heavier to solve. 2D models can give new information on local phenomena.

2D models are still widely used, as 3D models are either unnecessary or impractical for studying many fuel cell phenomena. Some examples can be seen in, e.g., [52, 53]. A typical 2D model focuses on transport phenomena in the membrane and GDLs or local current distribution.

Three-dimensional cell models

3D models are often the most realistic ones as the cell geometry can be modelled more or less exactly as it is, although many other simplifications still have to be made. However, this also means that solving these models takes more computer capacity and time. 3D models are at their best when studying phenomena that cannot adequately be modelled in 2D such as reactant flow and distribution. A 3D model can be used to gain information on whether the reactants are distributed evenly across the whole cell or the current distribution of the cell is uniform.

Many 3D models such as the early examples presented in [54–56] exclude the MEA or the electrodes, as these are very thin layers and greatly increase the size of the computational grid in a 3D model. It is also typical not to study the whole cell or flow field but only part of it, such as one turn of a serpentine channel, i.e., to take advantage of possible repeating units and symmetry. There are also models that cover the whole active area of a small cell such as, e.g., [57], in which a 4×4 cm fuel cell was modelled to study the effects of different channel cross-sections on the performance of the cell. It is problematic that even the so-called large-scale models are models of relatively small cells, e.g., 7×7 cm^2 in [32]. Apart from the smallest applications, most real world cells will have much larger active areas to produce the necessary amount of power. The problem lies in the fact that flow field behaviour is not scalable and channel geometry that works well in small cells may therefore not perform as well in a larger cell, as the Reynolds number does not remain constant when the cell size changes. Thus, more effort should be made to model cells that could actually be used in stacks instead of those that are only used in laboratories, especially as the modelling

work done so far has shown that the flow field design is crucial to good cell performance.

Dynamic models

A dynamic model is one that includes the time dimension, i.e., in which cell operation is not constant but has a time dependency. Thus, dynamic models can be used to predict responses at the cell, stack or system level to changes or disturbances in operating conditions. Dynamic modelling is a good tool for studying performance during start-up, shutdown and voltage cycling, see, e.g., [58].

Dynamic models are typically dependent on empirical correlations (see, e.g., [59]), as including the time dimension requires significantly more computing capacity and time than is necessary for solving a steady-state model as, for example, the cell may be modelled using an equivalent circuit (such as presented in, e.g., [60]) that consists of a few electrical components such as resistors and capacitors connected so that the circuit behaves similarly to a fuel cell. This makes the models considerably simpler. Thus, in many cases the cell itself is not the point of the study, as the model focuses on the system, such as in [61]. Dynamic models that use physical and electrochemical correlations can give estimations of, e.g., how quickly the cell reaches steady-state operation after changes in operating conditions, see, e.g., [62, 63].

Two-phase models

One of the most challenging aspects of PEMFCs, both in terms of modelling and operating the cell, is water management. As discussed in Section 2.3, liquid water is necessary for the ionic conductivity of the membrane, but when too much of it accumulates in the electrodes, it obstructs mass transport to and from the reaction sites. Thus, water management is crucial in terms of cell performance.

There are two usual methods for modelling two-phase mass transport. One is known as the multiphase mixture model. In it, the two phases are considered a mixture for which the equations are solved, see, e.g., [64–66]. The data for each phase can then be calculated from the mixture solution. In the second approach, the multifluid model, both phases have a set of equations and both sets are solved simultaneously, see, e.g., [67, 68]. The latter method requires more computational capacity and a more efficient solver, as convergence is relatively difficult to attain, but it also gives more accurate results and predictions on phenomena that are unachievable using the other method. Both models work only

with porous media flow, i.e., when Darcy's law applies, and thus should not be used for modelling the two-phase behaviour in gas channels. This is problematic because water accumulation is a process that should definitely also be studied in 3D and across the whole flow field, not just as a cross section of the GDLs and MEA.

There are some experimental techniques, such as neutron imaging technology, see, e.g., [69], to study water transport and accumulation in the cell, but accurate two-phase models would be a great help in understanding and improving PEMFC water management. Many parameters for two-phase models are chosen almost arbitrarily or are derived from results of experiments performed with soil. Perhaps the most significant of these is capillary pressure for which various relations that differ significantly[3] have been used. It should also be mentioned that many two-phase models use inaccurate boundary conditions such as that at the boundary between the channel and the GDL, there is no liquid water (i.e., all water is gaseous), see, e.g., [54, 70]. This is clearly inaccurate, as many experiments have shown droplet formation in channels, see, e.g., [71]. Some studies suggest novel boundary conditions as a solution to this problem, for example, by using a basic model for droplet formation on the boundary, see, e.g., [72, 73]. However, liquid water transport in the channels, which affects the evaporation from this boundary, has never been modelled accurately, as Darcy's law does not apply in the channels and thus neither do the two-phase models presented in the fuel cell literature. Considering these issues, it is clear that two-phase modelling requires many improvements before the results can be trusted.

3.2 Modelling in This Thesis

The modelling done in this thesis focuses on gaining a better understanding of the following subjects:

- mass transport phenomena on the cathode (in Publications 1 and 5)
- the effect of thermal and electric contact resistances on local cell phenomena (in Publications 2 and 3)
- compression distribution in a stack (in Publication 4) that strongly affects the contact resistances.

[3] As an example, compare the formulations for capillary pressure used in [57] and [59].

These studies are described in the following sections. The subject under study varies between the models, but all the modelling work shares the common aim of trying to see beyond the IV-curve, i.e., studying local or cell-scale phenomena in an operating fuel cell that normally remain invisible.

Using the categories of the FC model presented in the previous section, the models made as a part of this thesis can be divided into 2D and 3D models. Two of the 2D models are cross-sectional for studying the effect of compression, contact resistances and GDL deformation discussed in Chapter 5 and Publications 2 and 3. These models study the local effects that the uneven compression resulting from the cell structure causes to the current density distribution and other variables. Another 2D model focuses on the cathode of a free-breathing fuel cell. It differs slightly from typical 2D FC models in that it includes the ambient air zone. This model was used to study the optimal way to model such a cell and, based on the results, a computationally light 3D model of a free-breathing cell was built. The 3D model was then used to study the effect of cell size and orientation on the effectiveness of the natural convection phenomenon. The free-breathing call model is presented in Publication 5 and Chapter 7.

A 3D model was built to study the flow distribution in a parallel flow field, i.e., a flow field in which continuous parallel channels cross the active area of the cell (Chapter 4 and Publication 1). This model was used to optimize the flow field geometry so that a more even flow distribution was attained. Another 3D model focused on the compression distribution in a stack (Chapter 6 and Publication 4) and was used to improve the end plate structures so that the compression distribution in the cell was limited to a suitable range.

COMSOL Multiphysics, the commercial differential equation solver software, was used in the modelling. It is based on the finite element method (FEM) in which the modelling domain is discretized to finite elements and the equations are solved in each element using piecewise continuous polynomials. A more detailed description of FEM can be found in, e.g., [74]. COMSOL is sophisticated software that is capable of creating the mesh for complex geometries and offers various solver algorithms for different types of problems.

3.3 Modelling Principles

The purpose of this section is to present the physics and electrochemistry employed in this thesis. Each of the models presented in the later sections includes only the equations essential to the subject of study. However, the underlying

physics is always the same. A general view of the physics used in the models is given in this section, and the details of each model are explained in the corresponding chapter. The modelled FC phenomena consist of mass, heat and charge transfer, electrochemical reactions, compression effects and pressure distribution. These are modelled with suitable partial differential equations and boundary conditions, depending on the model. The coupled partial differential equations are presented in the following sections.

3.3.1 Mass Transfer

The modelling of mass transfer consists of modelling the transport of reactants, reaction products and inert substances in the fuel cell. In a PEMFC, the reactants are hydrogen on the anode and oxygen on the cathode, and the reaction product is water. The inert phase is nitrogen, or a mixture of nitrogen and argon. Both these gases are present in air and thus in the cathode of a fuel cell operating on air. They do not participate in reactions but do affect the mass transport inside the cell. In this thesis, water is assumed to be in the vapour phase, as two-phase modelling, due to its complexity and inaccuracies as discussed in Section 3.1, was beyond the scope of this work. Anode mass transport is excluded from the models, however, as performance-limiting phenomena usually occur on the cathode due to the slower reaction kinetics and increased risk of flooding. In this thesis, mass transport modelling focuses on the distribution of reactants on the electrode, on the one hand studying the flow field on the scale of the entire cell, and, on the other hand locally on the scale of individual ribs and channels.

Species are transported on the cathode through convection and diffusion. An externally supplied pressure difference across the cell creates a flow through the cell, or, in the case of free convection, the lift produced by density variations in air, in turn, caused by temperature and concentration differences. On the electrode, the reactants are consumed and reaction products generated, which creates concentration gradients in addition to the density gradient. The fluid flow passes through the channels, the porous gas diffusion layer and the electrode. The membrane is impermeable to gases but can transport water. Membrane water transport is not the focus of this thesis, however, and has been modelled with a simple empirical correlation.

In the channels, the fluid flow is modelled with the Navier–Stokes and continuity equations (8) and (9). These are standard equations for modelling laminar, incompressible flow. There is no exact limit for the change from laminar to tur-

bulent flow, but fluid flow can usually be considered laminar if the Reynolds number for that flow is below 2300. This condition is met in the fuel cell environment in which the flows are relatively slow. In the porous gas diffusion layer and the electrode, however, Darcy's Law (10) is used instead.

$$-\rho\mathbf{u}\cdot\nabla\mathbf{u}+\rho\mathbf{g}-\nabla p+\nabla\cdot\left(\eta(\nabla\mathbf{u}+\nabla\mathbf{u}^{\mathrm{T}})\right)=\mathbf{S}_{NS} \tag{8}$$

$$\nabla\cdot(\rho\mathbf{u})=S_{con} \tag{9}$$

$$\nabla\cdot\left(\rho\frac{\eta}{\kappa}\nabla p\right)=S_D \tag{10}$$

Here, ρ is the average density of the fluid, $\mathbf{u}(u,v,w)$ the (mass average) velocity vector, p the pressure, κ the permeability of the porous medium, S the source term of each equation and η the average viscosity of the fluid.

Equations (8–10) model the behaviour of the fluid in terms of pressure and velocity in a centre of mass frame. In order to take into account the effect of concentration-driven flow, diffusion must also be modelled. The use of the simple diffusion equation (i.e., Fick's Law) is incorrect in a fuel cell cathode, however, as the fluid has three components (oxygen, water and nitrogen) that all have different sources, sinks and diffusion constants. Thus, multicomponent diffusion equations, or Maxwell–Stefan diffusion equations (11) and (12), must be employed. It should be noted that although the Maxwell–Stefan equations can be written for each component, they only need to be solved for two, as the third component can always be calculated from the other two, as the mass fractions must add up to one. Thus, the mass fraction of nitrogen is calculated from those of water and oxygen.

$$\nabla\cdot\left(-\rho\omega_i\sum_{j=O_2,H_2O,N_2}\tilde{D}_{ij}\left(\nabla x_j\right)+\rho\omega_i\mathbf{u}\right)=S_i^{mass},\qquad i=\mathrm{O_2},\mathrm{H_2O},\mathrm{N_2} \tag{11}$$

$$\nabla x_j=\frac{M^2}{M_j}\sum_{\substack{k=O_2,H_2O,N_2\\k\neq j}}\left(\frac{1}{M}+\omega_k\left(\frac{1}{M_k}-\frac{1}{M_j}\right)\right)\nabla\omega_k \tag{12}$$

Here, ω_i is the mass fraction of species i, $\tilde{D}_{\mathrm{ij}}$ the Maxwell–Stefan diffusion coefficient, M_i the molar mass and x_i the molar fraction of species i. Maxwell–Stefan equations can also be written for molar fractions (as opposed to mass fractions):

$$\nabla \cdot (c x_i \mathbf{u}) - \nabla \cdot \left(c \tilde{D}_{eff} \nabla x_i \right) = S_i^{molar}, \qquad i = \mathrm{O_2}, \mathrm{H_2O}, \mathrm{N_2} \tag{13}$$

The formulations (11) and (13) are equivalent. More information on the Maxwell–Stefan equations can be found in, e.g., [75]. Both forms have been used in this thesis.

The source terms S in equations (8–11) and (13) arise from the cell reactions, which consume oxygen and produce water. Thus, they only exist in the electrodes and are zero elsewhere. The exceptions to this are the source terms in the Navier–Stokes and continuity equations that are only used in the flow field model discussed in Chapter 4 and Publication 1, in which the only modelled cell component was the flow field and thus the effect of the reactions modelled as though the reactions occurred in the channels.

$$\mathbf{S}_{NS} = -\frac{jA}{zFV_{ch}} M_{O2} \mathbf{u} \qquad \text{(for Navier–Stokes eq.)} \tag{14}$$

$$S_D = \frac{j}{4F} \left(M_{H2O} - M_{O2} \right) \qquad \text{(for Darcy's Law)} \tag{15}$$

$$S_{con} = \frac{jA}{zFV_{ch}} \left(\alpha M_{H2O} - M_{O2} \right) \qquad \text{(for continuity eq.)} \tag{16}$$

$$S_i^{mass} = \begin{cases} -\frac{j}{4F} M_{O2}, & i = \mathrm{O_2} \\ \frac{j}{2F} M_{H2O}, & i = \mathrm{H_2O} \end{cases} \quad \text{and} \quad S_i^{molar} = \begin{cases} -\frac{j}{4F}, & i = \mathrm{O_2} \\ \frac{j}{2F}, & i = \mathrm{H_2O} \end{cases}$$

(for Maxwell–Stefan diffusion equation) (17)

Here, j is the reaction current density at the electrode, A the active area of the cell, z the number of electrons participating in the reaction, F the Faraday number, α the portion of reaction product water leaving the cell through the anode[4] and V_{ch} the volume of the channels.

[4] A portion of the reaction product water can be driven from the anode to the cathode by diffusion.

3.3.2 Heat and Charge Transfer

PEMFCs operate at a lower temperature than other fuel cells such as SOFCs, but heat transfer is nevertheless an essential factor for cell performance. In this thesis, the focus is not on cell or stack thermal management but on local differences in temperature. For example, local temperature variations, i.e., often called hot spots, may be formed due to the rib/channel structures and uneven current density. These do not affect the cell performance very much but can cause premature membrane degradation and thus shorten the lifetime of the cell.

The modelling of heat transfer is fairly straightforward. There are two mechanisms of heat transfer in the cell: convection and conduction. Heat transfer by radiation is usually not significant within a PEM fuel cell as the temperature and the thermal bulk and contact resistances are relatively low. Heat transfer is modelled using equation (18):

$$\nabla \cdot (k \nabla T) = \sum_i c_{p,i} \rho_i \mathbf{u} \cdot \nabla T + S_T \tag{18}$$

Heat is produced by the cell reactions and ohmic heating by electronic and ionic current. Thus the thermal source term S_T in each region is

$$S_T = \begin{cases} \sigma^s_{GDL} \left(\nabla \Phi_s\right)^2, \text{in the GDLs} \\ \sigma^m_{mem} \left(\nabla \Phi_m\right)^2, \text{in the membrane} \\ \sigma^s_{CL} \left(\nabla \Phi_s\right)^2 + \sigma^m_{CL} \left(\nabla \Phi_m\right)^2 + j_a \eta_a + \dfrac{j_a T \Delta S_a}{2F}, \text{ in the anode} \\ \sigma^s_{CL} \left(\nabla \Phi_s\right)^2 + \sigma^m_{CL} \left(\nabla \Phi_m\right)^2 - j_c \eta_c - \dfrac{j_c T \Delta S_c}{4F}, \text{ in the cathode} \end{cases} \tag{19}$$

Here, σ is the electronic or ionic conductivity of the GDL for membrane (*mem*) and catalyst (*CL*), Φ_m and Φ_s the ionic and electronic potential, η_a and η_c the overpotentials of the anode and cathode, j_a and j_c the reaction current densities at the anode and cathode, T the temperature and ΔS the change in entropy of the reaction. Note that as j_c is negative, the cathode side source terms have negative signs before the source terms.

The charge transfer in a PEMFC comprises the movement of both electrons and ions. Thus, it is necessary to model both ionic and electronic potential separately. The former exists only in the membrane and electrodes while the latter

exists in the electrodes and GDLs. The charge transfer, ionic or electronic, is modelled by

$$-\nabla \cdot \left(\sigma_{mem,GDL} \nabla \Phi_{m,s}\right) = S_{m,s} \tag{20}$$

The conductivity $\sigma_{mem,GDL}$ is a function of membrane humidity. The source terms, S_m for the ionic potential and S_s for the electronic potential, are non-zero in the electrodes:

$$S_m = \begin{cases} j_a \text{ , anode} \\ -j_c \text{ , cathode} \end{cases} \text{ and } S_s = \begin{cases} -j_a \text{ , anode} \\ j_c \text{ , cathode} \end{cases} \tag{21}$$

The reaction current densities j_a and j_c at the electrodes are calculated according to equation (D) presented in Section 2.5.

An interesting aspect of heat and charge transfer in a fuel cell is that these variables are, in reality, not continuous between different cell components. This is due to contact resistances between the components, e.g., between the GDL and the electrodes. These contact resistances have spatial variation, as the compression applied to these components varies on the scale of the whole active area and locally under the ribs and channels. The differences in thermal and electric contact resistances can have a significant effect on cell performance and lifetime, which is discussed in Chapter 5 and Publications 2 and 3.

3.3.3 Mechanical Modelling

The equations presented in the last two sections are all transfer equations and are used in similar models. This thesis also includes a study of the compression distribution in a stack, which is discussed in more detail in Chapter 6 and Publication 4. Compression is modelled by solving equation (22) in the whole modelling domain with appropriate boundary settings.

$$\nabla \cdot \sigma_{str} = 0. \tag{22}$$

Here, $\sigma_{str} = (\sigma_x, \sigma_y, \sigma_z, \tau_{xy}, \tau_{yz}, \tau_{xz})^T$ is a stress tensor in which normal stresses are marked with σ_i and shear stresses with τ_{ij}. The stress tensor is related to the strain tensor $\gamma = (\gamma_x, \gamma_y, \gamma_z, \gamma_{xy}, \gamma_{yz}, \gamma_{xz})^T$ by Hooke's law:

$$\sigma_{str} = D\gamma \tag{23}$$

where D is the elasticity matrix calculated using Young's modulus and Poisson's ratio:

$$D = \frac{E}{(1+\upsilon)(1-2\upsilon)} \begin{bmatrix} 1-\upsilon & \upsilon & \upsilon & 0 & 0 & 0 \\ \upsilon & 1-\upsilon & \upsilon & 0 & 0 & 0 \\ \upsilon & \upsilon & 1-\upsilon & 0 & 0 & 0 \\ 0 & 0 & 0 & \frac{1}{2}-\upsilon & 0 & 0 \\ 0 & 0 & 0 & 0 & \frac{1}{2}-\upsilon & 0 \\ 0 & 0 & 0 & 0 & 0 & \frac{1}{2}-\upsilon \end{bmatrix} \tag{24}$$

The strain ε is a measure of the material's deformation, i.e., the change in length at a certain point divided by the original length at that point. The components of the strain tensor ε are calculated by

$$\gamma_i = \frac{\partial \mathbf{u}_i}{\partial i}, \ \gamma_{ij} = \frac{\partial \mathbf{u}_j}{\partial i} + \frac{\partial \mathbf{u}_i}{\partial i}, \ i, j = x, y, z \tag{25}$$

where $\mathbf{u} = u\mathbf{i} + v\mathbf{j} + w\mathbf{k}$ is the deformation vector.

Using these equations, the following differential equation can be written for the deformation:

$$\nabla \cdot (D\nabla \mathbf{u}) = 0, \tag{26}$$

which is the differential equation solved. This model assumes that all materials are isotropic, homogeneous and elastic. The boundary conditions are simple: an inward force is applied to areas corresponding to the locations where nut and bolt assemblies are in the stack. The stack geometry was symmetric, so only one eighth of the structure had to be modelled. Thus, there are some symmetry boundaries at which the material is assumed to be immobile in the normal direction. Other boundaries may move freely.

4. Flow Field Modelling

Here, the aim of flow field modelling is to study the velocity profile, reactant and reaction product distribution in a fuel cell and thus determine which kind of flow field is optimal for a given fuel cell structure. As discussed in Section 2.3.3, there are a number of different flow field typologies as well as many changeable parameters, such as the channel dimensions and cross-sectional shape. Flow field behaviour does not scale with size, and thus a small fuel cell requires a different flow field design to a large one. Operating conditions, especially humidity and operating current, affect the water management of the cell and thus set their own requirements for the flow field. As a consequence, it is not possible to have a universally optimal flow field. Instead, the flow field should be designed separately for each application.

The most common problems of flow fields (in addition to the cost and weight of the bipolar plate) are uneven reactant distribution and insufficient liquid water removal. The former is typically due to poor flow field design and is common with the parallel channel configuration. The latter results from low flow velocities or generally poor flow field design and is harder to model, as two-phase modelling, in general, is not very exact and droplet formation and behaviour are difficult to predict. There have been experimental as well as modelling efforts concerning liquid water removal in the bipolar plate, see, e.g., [76–78], but in this thesis the focus is on improving the reactant distribution.

There are three common approaches to designing a channel system for a PEMFC. The first is to have several parallel channels across the active area. The second is to have a few channels, or just one long channel, that cover the active area by twisting and turning (serpentine channels). The third is to have dead-end channels that force the flow into the GDL (interdigitated channels). For a more in-depth explanation of these three and other flow field types, see, e.g., [79]. The parallel channel system, the focus of this thesis, has often been criticized for

unequal flow velocities in the channels, thus causing uneven reactant distribution. It also has a low pressure drop across the cell, however, which means that less capacity is required from auxiliary equipment such as pumps, though this may also make water removal less effective. With serpentine (or interdigitated) channels, it is easy to accomplish an even flow distribution as there are only a few channels, which has led many to prefer these configurations over the parallel one.

This thesis focused on studying the parallel channel configuration and thus showing that it can be used effectively as long as the flow field design is optimized. By modelling the cathode of a PEMFC, it was demonstrated that the crucial detail is the way the flow is distributed into the channels. In order to illustrate this concept, a basic parallel channel system is presented in Figure 4.

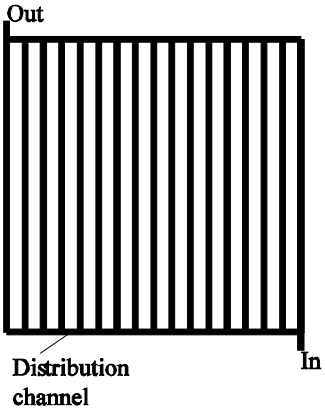

Figure 4. A schematic of a typical parallel flow field design.

Here, the distribution channel has the same width as the other channels. This is not an optimal solution, however, as the resulting flow distribution tends to be uneven. In order to study the effect of the distribution channel shape or, more accurately, its hydraulic resistance to the flow distribution, the existing cell geometry was taken as a starting point. This geometry is illustrated in Figure 5. This is a channel system in which the channels form groups of five in a 3D structure and the distributor channel has a slightly more complex geometry, but the parallel channel principle is the same as in Figure 4.

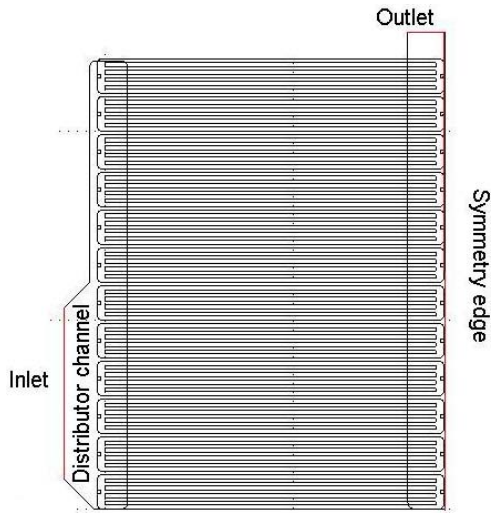

Figure 5. Starting point geometry for flow field modelling. As the structure is symmetrical, one half of the channel system is modelled with one boundary functioning as a symmetry boundary.

The flow field of this geometry was modelled using the Navier–Stokes equations (8) and the continuity equation (9). At the inlet, velocity was set to correspond to a stoichiometry of 1.2 and, at the outlet, the pressure relative to the inlet was set to zero. Thus the real pressure can be calculated by adding atmospheric pressure. The reason for not using atmospheric pressure as a boundary condition is that it is several orders of magnitude larger than the pressure variations within the model, and thus using it may create unnecessary numerical problems in the solution process. Due to the symmetry condition, one boundary had the symmetry boundary condition, i.e., the normal velocity and viscous stress at that boundary were set to zero. The remaining boundaries had the so-called no-slip condition, i.e., the velocity was set to zero.

The effect of the cell reactions to the fluid composition was taken into account by adding source terms to equations (8) and (9) according to equations (14) and (15). The density and viscosity of the fluid were calculated from the composition of the gas mixture and thus vary within the modelling domain. Equations (14) and (15) are based on the assumption that the momentum of the reactants consumed in the reactions is lost to the porous media. This may not be completely correct, and thus alternative source terms for which the momentum was conserved in the flow were also modelled. The results showed that the relative dif-

ference in flow velocities between the models using these source terms was negligible at 0.1%.

It should be noted that all water was assumed to be in gaseous form. The relative humidity of the gas mixture was calculated from the solution and had a maximum value below 100% if the relative humidity of the inlet flow was a maximum of 64%. Thus, there is no water condensation with the boundary conditions used here (21% inlet relative humidity corresponding to typical operating conditions). However, this does not hold true for all PEMFC operating conditions, and thus the model could be developed further if two-phase phenomena could be modelled accurately. In this case, two-phase modelling is more complicated than usual as the widely used relations are developed for porous media and do not apply to channels.

The modelling of the geometry presented in Figure 5 showed that the flow distribution in the channels was uneven, with the flow velocity in the fastest channel being 16% higher than in the slowest channel. The flow field geometry was altered with a trial and error method. The key to improving the flow distribution proved to be changing the flow resistance of the inlet distributor channel. This was done by narrowing the end of the distributor channel, as the highest channel velocities had been formed at the channels starting from the end of the distributor channel. The changes made to the distributor channel are illustrated in Figure 6.

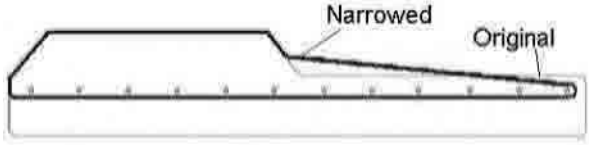

Figure 6. The original and modified distributor channel geometries.

The relative channel velocities of the original and modified geometries are illustrated in Figure 7. Although the original distribution was quite good, it was further improved by the changes made to the distributor channel.

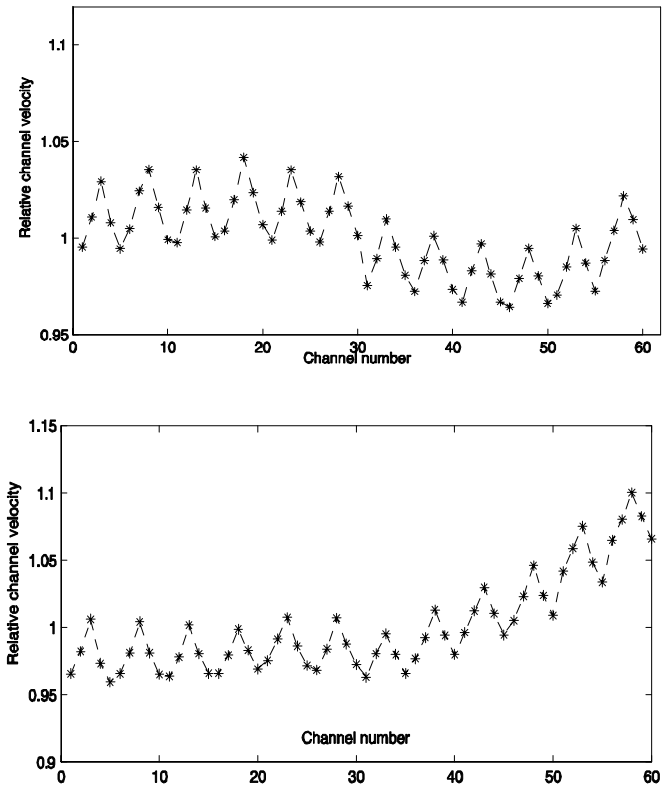

Figure 7. Flow velocities in the channels with the original (left) and modified (right) distributor channel.

The modelling results were validated experimentally by observing the progress of ink dispersed in water in the channels. Flow velocity was calculated from video images by working out the time an ink pulse required to traverse each channel. The flow field size and flow velocity were scaled in order to reach a corresponding Reynolds number. The fluid was changed from gaseous to liquid for practical reasons. The measurement accuracy was not sufficient for quantitative results, but qualitatively the experimental results were in agreement with the modelling results and confirmed that the improved geometry gives a more even flow distribution. Originally, the purpose was to employ the improved geometry in a stack and see if performance improvement could be perceived. This was never done, however, as the research project of which this work was part abandoned the stack development in favour of using a commercial stack, and to perform the experiment just to validate the model would have been too expensive.

The main result from the flow field modelling was that parallel flow fields can have sufficiently even flow distribution, contrary to some claims. The flow field design can be significantly improved by fairly simple modelling, and excluding thin components such as GDL and MEA makes it possible to model larger channel systems such as would be used in a real stack. The inlet distributor channel should be designed individually for each flow field using modelling as an optimizing tool in order to improve performance.

5. Contact Resistance Modelling

A significant part of the ohmic losses in a fuel cell arises from the contact resistances between different components, most importantly between the gas diffusion layer and its adjacent components: the electrodes and the bipolar plate ribs. By reducing these contact resistances, the cell performance can be improved. The subject of the GDL contact resistance has been studied in, e.g., [80, 81], but two factors are not included in their studies. Firstly, compression affects the bulk conductivity as well as the porosity, thermal conductivity, permeability and water transport properties of the GDL. Thus, finding the optimal compression is not a straightforward matter but requires finding the compromise that best suits these conflicting factors. Secondly, the compression within a fuel cell is not constant. On the one hand, the compression is applied to the cell or stack through end plates using a nut and bolt assembly. The variations in compression due to this mechanism are discussed in the following chapter, but here it is sufficient to note that the size of these variations can be large, if the cell design is not optimal. On the other hand, there are notable local variations in the GDL compression due to the alternating rib/channel structure of the flow field plates.

The study of the effect of local variations was the point of interest in Publications 2 and 3 and is discussed in this chapter. The model developed for this purpose consisted of a cross-section of the cell, one half of it beneath a channel and the other half beneath a rib. As little data were available on the dependencies, parameters such as the GDL thermal and electrical conductivity and the contact resistance between the GDL and the electrodes under compression were experimentally measured by others in the laboratory and the results were published in [82]. Based on these results, a model using compression-dependent parameters for permeability, porosity and electrical conduction was built and presented in Publication 2. This model gave some interesting results, especially with regard to local current distribution, for which the model predicted a sharp peak in the catalyst layer beneath the rib/channel edge. Such a peak could lead to the creation of a hot spot and thus membrane damage.

The model presented in Publication 2 was isothermal, however, and thus could not give data on the temperature distribution. The contact resistance between the GDL and the catalyst layer had been assumed to have a simple correlation with the contact resistance between the current collector and the GDL. In reality, the GDL is free to deform under the gas channel. Thus, the compression distribution between the GDL and electrode may not be equal to the one between the GDL and the bipolar plate. Furthermore, the correlation between compression and contact resistance is not necessarily the same for these pairs as the solid and smooth surface of the BP is quite different to that of the microporous electrode. Consequently, new experiments were conducted and the results published in [83]. These results were incorporated into the model in Publication 3 along with the heat conduction equation (18). With these more accurate parameters, the current density peak was lower though still in existence. The modelling domain is illustrated in Figure 8, along with the model that is typically used, which assumes the GDL is a uniform block of constant thickness and was used as a base case for comparison in this study.

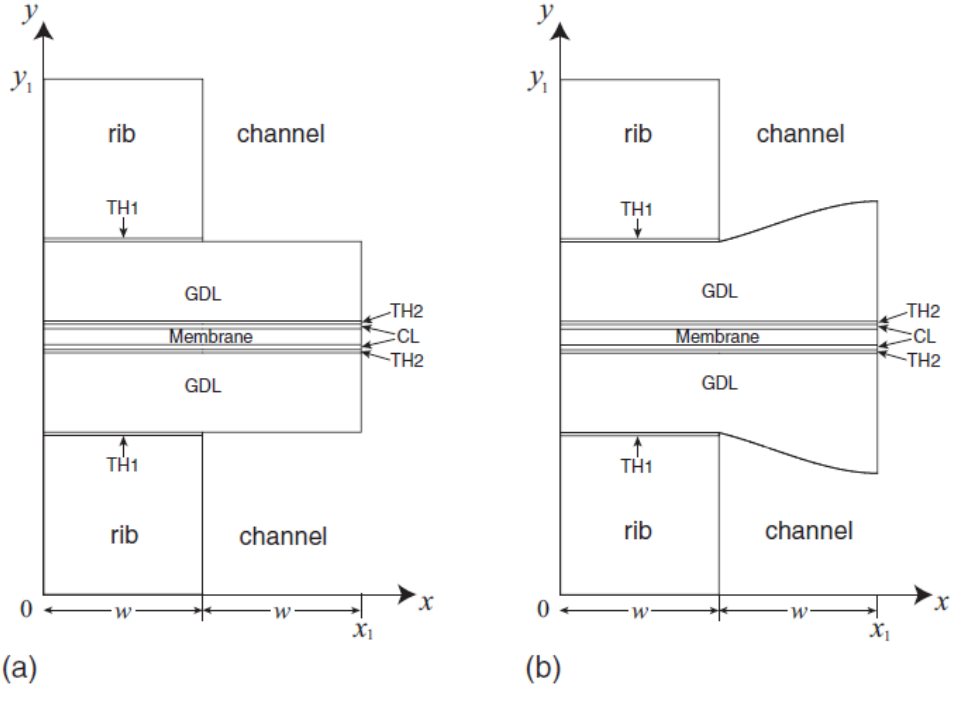

Figure 8. The base case (a) and the contact resistance variation model (b) (pictures by Iwao Nitta, Publication 2).

Current density distributions of the variable contact resistance model and the base case model are illustrated in Figure 9. The perpendicular current density at the GDL/electrode boundary is illustrated further in Figure 10. Here, it is easy to see the increase in current density beneath the rib/channel boundary. The current density distribution is clearly not constant locally, as has been assumed in many earlier models, but can have large local variations. The variation in current density is due to the large amount of lateral current density. The current generated in the reactions under the channel is conducted to the BP through the portion of electrode under the rib, as the contact resistance between the electrode and the GDL is much lower under the rib, and the current is always conducted through the path of least resistance. The current density peak effect is, in practice, impossible to discern from the overall cell performance. However, it can cause lifetime issues if the electrodes and MEA are damaged by the resulting temperature variation. Furthermore, if the poor contact resistance under the channel could be improved, the overall performance of the cell could also show improvement.

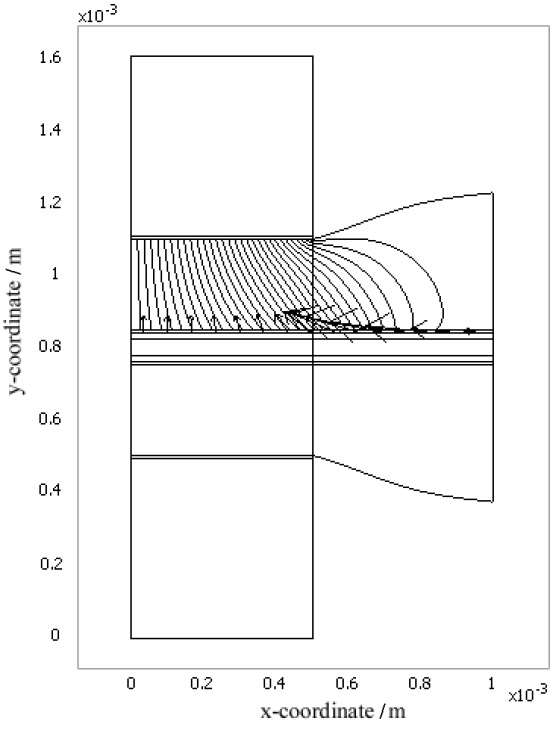

Figure 9. The model geometry of the contact resistance model and the current density in the cathode. The arrows show the direction of the current while the lines are potential level curves. There is a large lateral current in the catalyst layer beneath the channel where the contact resistance between the GDL and the electrode is high. (Picture by Iwao Nitta, Publication 3.)

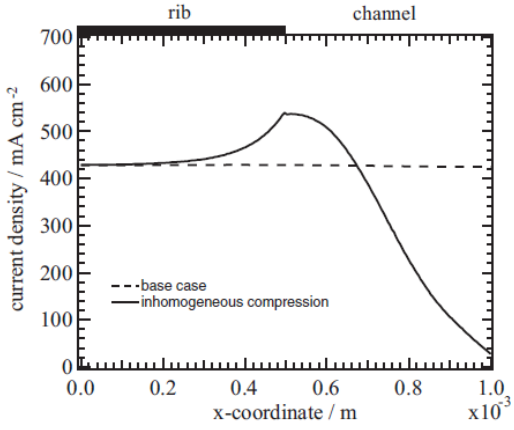

Figure 10. The perpendicular current distribution at the GDL/electrode boundary (picture by Iwao Nitta, Publication 3).

The main result of the contact resistance modelling was that local changes in compression that result in contact resistance variation can have a significant effect on the local current density distribution. Large current density variations can cause damage in the long term through ohmic heating and temperature variation. The large contact resistances under the channels that force the current to travel within the electrodes can also result in ohmic losses.

6. Modelling the Compression Distribution in a Stack

The previous chapter discussed the effect of compression in a fuel cell on a small scale. This chapter focuses on a related matter, i.e., studying how compression is distributed throughout the stack and the individual cells in the stack. The motivation is obvious: the contact resistance experiments indicate that many critical parameters such as the contact resistances and the GDL bulk transport properties are very sensitive to compression. Based on literature, the ideal compression range seems to be approximately 10–30 bar depending on the materials [84–86], with 10–15 bar being optimal for a typical cell.

The distribution of compression in a stack was studied by taking an existing stack as a starting point. The stack was modelled with five unit cells, a number that was decided as large enough to simulate a real stack but small enough that the model could be solved with the available computing capacity. Symmetry boundaries were used to further decrease the heaviness of the model. The end plate geometry is illustrated in Figure 11. The modelling domain consisted of end plates, bipolar plates, gaskets and an averaged layer representing the GDLs and MEA, which could not be modelled as separate layers as they are thin layers and would thus require a very fine mesh. The compression was directed to the end plates via circular boundaries corresponding to the nut and bolt assembly. The end plates were steel plates of constant thickness.

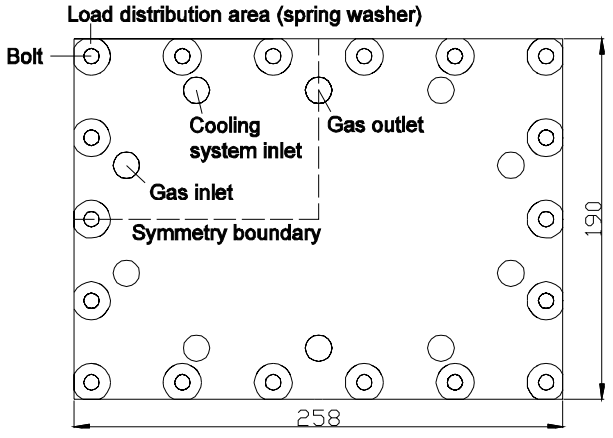

Figure 11. The end plate geometry and symmetry boundaries. The dimensions are in millimetres.

The results showed that, in this case, the compression distribution is quite far from optimal, as can be seen in Figure 12, which displays the pressure on the GDLs of the middle cell in the stack. Most the active area experiences pressure below 10 bars and the centre parts even lower than 2 bars. In an operating fuel cell, this pressure distribution can be expected to lead to problems with contact resistances, thus lowering the performance.

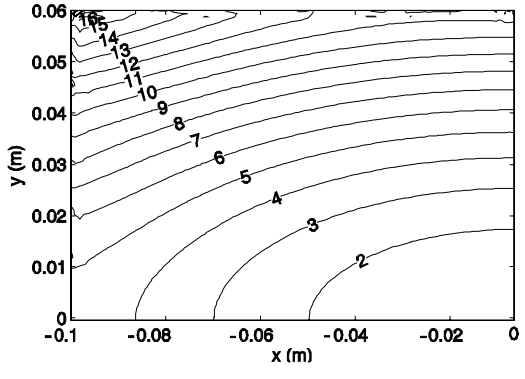

Figure 12. The clamping pressure isobars on the GDL surface of the original flat plate (1 kN load at each bolt). The pressure values are in bars. The origin (lower right corner) is situated at the centre of the cell.

The problem is due to two main factors. Firstly, the force applied to the nuts and bolts was equal at each bolt, and due to their placement (see Publication 4) the corners of the plate experienced more pressure than the rest of the edges. Secondly, the uniformly thick steel plate is not rigid enough to distribute the pressure evenly and deforms slightly. Most of the pressure is directed to the gaskets. The end result is that while the corners of the active area are nearly crushed under almost 20 bar pressure, the centre areas of the cell experience only slight pressure at 2 bar or less.

Both factors were addressed in order to improve the pressure distribution. Different torques were applied to the bolts until a suitable configuration was found. The end plate structure was changed from a uniformly thick plate to a ribbed structure that also made the plate lighter. Further weight was lost by changing the end plate material to aluminium. While less rigid than steel, aluminium has other beneficial qualities, such as lower density. Aluminium is also easier to machine, which is important for future commercial applications. Figure 13 shows the compression distribution for different end plate configurations and materials. The best one is an aluminium plate with 7-cm-high aluminium ribs. Here, the pressure distribution remains within the ideal range of 10–15 bar.

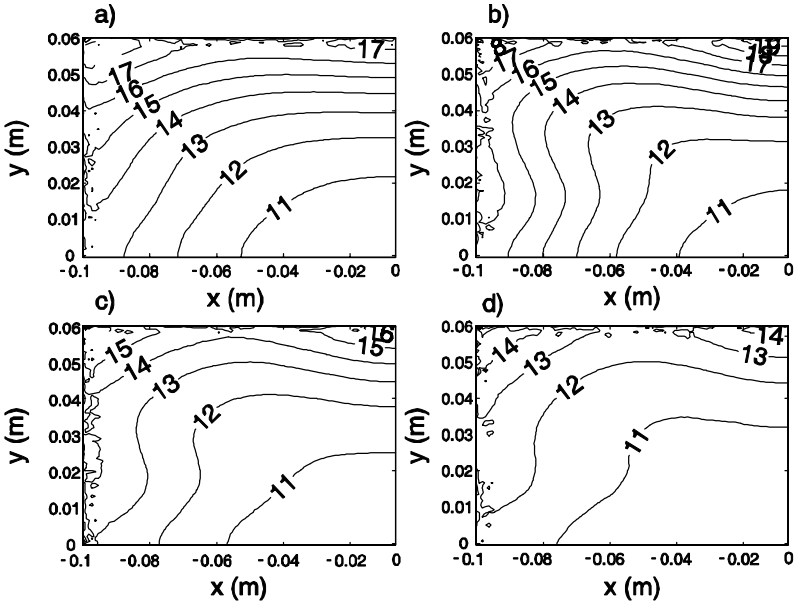

Figure 13. Pressure isobars on the GDL: a) 4 cm steel ribs, b) 5 cm aluminium ribs, c) 6 cm aluminium ribs and c) 7 cm aluminium ribs. The pressure values are in bars.

The experiments were also validated experimentally using a pressure-sensitive film. The accuracy and range of the film combined with rather large manufacturing tolerances in the stack components made the results more qualitative than quantitative however. Using the five cells in the stack resulted in mostly noise being measured, but using a single stack showed a clear correlation with the modelling results.

The main result of the stack compression modelling is that the compression distribution in a stack can be unacceptable if the stack has not been designed with care. The compression distribution can be significantly improved with fairly simple alterations however. Single cell units are more likely to suffer from uneven compression distribution as, in a large stack, the manufacturing tolerances, i.e., variations in the thickness of the components, can dominate the resulting compression distribution. These results should also be considered in the context of the previous chapter, i.e., the effect of compression on a local scale where noticeable effects on local current density distribution were observed. Large variations in cell compression may lead to surprising local effects, such as very high electrical and thermal contact resistances or greatly reduced mass transport capabilities that affect cell performance and lifetime.

The compression model created in this work was further developed by others in the laboratory, see, [87, 88]. The improvements there include adding a compression equalizing layer made of a flexible material and including the effect of thermal stresses in the model.

7. Modelling a Free-breathing Fuel Cell

This chapter and Publication 5 focus on modelling the mass transfer on the cathode of a free-breathing PEMFC. The objective was to create a computationally light but valid 3D model. This was done in two steps, first a 2D model was built for testing different approaches to the modelling and then a 3D model was built according to these results. The 3D model was then used to study briefly the effect of size and position on cell performance.

Models of free-breathing fuel cells have been built before, see, e.g., [89, 90]. As these studies do not describe in detail how they chose their model boundary settings and other such details, it was decided to start the model building by trying out different choices to see their effects on the result. The two main issues to be solved with the 2D model were the type of boundary setting that should be used and how large the ambient air zone, a.k.a. free convection zone of the model (see Figure 14), should be.

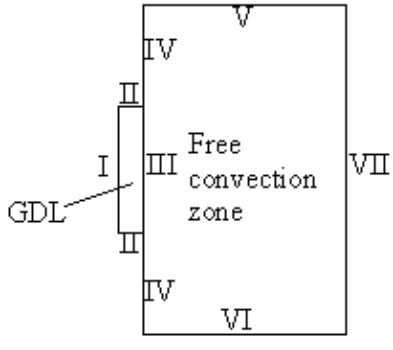

Figure 14. A schematic of the modelling domain in 2D. Note that the picture is not to scale.

The issue of boundary setting stems from the fact that there are two ways to model a free convection problem such as this one: the closed and the open boundary settings approaches, see, e.g., [91] for open and [92] for closed.

Mathematical formulation for the open boundary conditions:

$$\mathbf{t} \cdot \mathbf{u} = 0$$
Boundaries V, VI and VII: free convection zone boundaries (27)

$$\mathbf{n} \cdot (\mathbf{J}_i + \rho\omega_i\mathbf{u}) = \mathbf{n} \cdot \mathbf{u}\rho\omega_i \quad \text{(Boundary V)} \tag{28}$$

$$\omega_{O_2} = \omega_{O_2}^0 \,,\ \omega_{H_2O} = \omega_{H_2O}^0 \quad \text{(Boundaries VI and VII)} \tag{29}$$

$$T = T_0 \quad \text{(Boundary VII)} \tag{30}$$

For the closed boundary conditions:

$$\mathbf{u} = 0$$
Boundaries V, VI and VII: free convection zone boundaries (31)

$$\omega_{O_2} = \omega_{O_2}^0 \,,\ \omega_{H_2O} = \omega_{H_2O}^0 \quad \text{(Boundaries VI and VII)} \tag{32}$$

$$T = T_0 \quad \text{(Boundary VII)} \tag{33}$$

The other boundary conditions can be found in Publication 5. The difference here is that the open mode allows for mass and momentum transport through the boundaries whereas the closed version does not. Species and thermal energy transport are allowed in both models. Earlier fuel cell models such as [89] have used the previous one, but the latter has typically not been used in free-breathing PEMFC models and there are usually no arguments as to why this particular choice has been made.

The sizes of the ambient air zones were selected so that enlarging them further had no significant effect on the solution. It is clear that the closed boundary setting model requires a much larger modelling domain due to the fact that the closed boundaries force a vortex-like flow to form, which requires more space to model. Thus, the open boundary setting model is much smaller. The modelling of both situations revealed that the results are equivalent in the area they share, i.e., the domain of the open boundary conditions model. The open boundary settings model is smaller and requires a smaller mesh, and it is thus easier to solve. It would also appear that solving the closed boundary settings model, in

addition to requiring a larger mesh, is also otherwise more time-consuming, as the vortex shape of the flow forces the solution algorithm to advance more slowly due to the higher complexity. Taking these observations into account, it is clear that the superior choice is the open boundary setting models, even if the one used in previous PEMFC models was the closed boundary settings model.

The 3D model was built using the open boundary conditions. The modelling domain of the 3D model is illustrated in Figure 15.

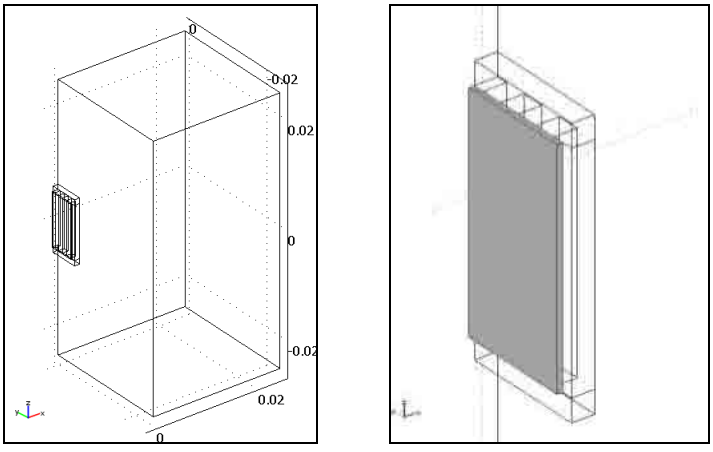

Figure 15. A schematic of the modelling domain in 3D with the cathode GDL and current collector ribs enlarged on the right. The shaded area represents the cathode GDL.

The results of the 3D model were compared with those of the 2D model and there were significant differences. The 2D model overestimates the mass transport by natural convection as it does not include the current collector ribs that obstruct the flow. This difference, less than 1%, is not significant for oxygen concentration on the electrode, but for water concentration it is approximately 10%. The 2D model also underestimates the heat transport as the current collector ribs are good heat conductors and increase the surface area of the cell and thus overestimates the temperature in the cell. The temperature difference between the models on the electrode is 6–8 K. The 3D model has a current density that is approximately 4% higher than that of the 2D model.

In this study, a 3D model that could later be used with experiments to optimize free-breathing fuel cell performance was created. However, the optimization is outside the scope of the work done here. This is largely due to the fact that before reliable results can be obtained with this type of modelling, two-

phase equations should be included, which in turn require some experimental work on various parameters. A few brief tests were performed with the model, however, to see the effect of cell size and positioning, i.e., the tilt angle on the performance. The modelled cell area (1 cm^2) was doubled and the current-voltage curves compared. The result was that there was no significant difference in the cell performance, indicating that in this small size range, natural convection is sufficient to provide the cell with reactants and remove reaction products. It was not possible to increase the cell size further with the available computing resources. Different tilt angles were also tested to determine the optimal positioning of the cell. Other related studies such as [85] have indicated that the cell performs best when it is positioned vertically, and this study confirmed these results.

8. Summary and Conclusions

This thesis focused on studying different aspects of PEMFC performance by modelling. These aspects include the dependence of contact resistances on compression and its effect on local cell performance, flow field behaviour in forced convection and free-breathing fuel cells as well as compression distribution in a stack. The modelling was done with Comsol Multiphysics, which uses the finite element method to solve partial differential equations. The results were experimentally validated when possible, although due to the nature of the modelling in this work and the practical limitations, the accuracy of the experimental results was mostly qualitative.

The flow field of the fuel cell cathode was studied by building a model of the cathode channel system. Other cell components such as the GDLs and MEA were excluded as they are very thin layers and would thus have increased the computational requirements too much. Crucially, these components also do not affect the flow field formation, although, in reality, the GDLs that extrude into the channels do affect the flow resistance. The flow field geometry was copied from an existing fuel cell and was a parallel channel system. The parallel channel system has often been seen as an inferior choice due to its tendency to cause uneven flow distribution, resulting in uneven reactant distribution on the electrodes and unsatisfactory cell performance.

In this work, it was shown that a correctly designed parallel channel system can have relatively even flow distributions. The key is to design the distributor channel so that it offers the necessary amount of hydraulic resistance. The distributor channel should be designed individually for each cell or stack depending on the operating conditions and cell size, as flow field behaviour is not scalable. The experiments were qualitatively validated by observing the progress of ink pulses in water flowing through the channel system, which allowed a flow velocity profile to be calculated. The experimental results were in agreement with the

modelling results, but the accuracy of the experiments was not sufficient for quantitative verification.

The effect of contact resistance on cell performance was studied using experimentally derived correlations for the dependency of contact resistance on compression. The compression in a cell varies on the scale of the whole cell and locally. This study focused on local phenomena. There are significant local variations in the compression that GDLs experience due to the alternating ribs and channels of the bipolar plates. Experimental results showed that the contact resistance between the GDL and electrode was especially dependent on the compression. This effect was modelled using a cross-sectional 2D model consisting of one symmetry unit, which was the width of one rib and one channel. This model was built in two phases, published separately, as the original results showed that there was a need for more accurate parameters, which were then acquired from experiments.

The results of contact resistance modelling show that the local current density is far from uniform, as there is a strong lateral current in the electrode layer. This is due to the fact that the contact resistance between the GDL and the electrode is large under the channel, and thus the current created in the electrodes, seeking the path of least resistance, travels through the electrodes until it reaches the portion of the contact boundary under the ribs where the contact resistance is smaller. The most important result is that there is a clear increase in current density in the electrode under the rib/channel boundary, which has not been observed or predicted in fuel cells before. This phenomenon can cause lifetime issues for the cell, although the model does not show a significant effect on the temperature distribution in the cell.

The experimental validation of this model was not performed, as an in-situ experiment to measure local current density would be very difficult to conduct and was not possible within the scope of this thesis. If, however, a way could be devised to perform these measurements, the results have the potential to be very interesting. It is known that membranes can develop small punctures, especially under high compression, temperature or current density, and it is possible that this lateral current mechanism and the ohmic heating it causes have an effect on this failure type. If so, the effect could possibly be mitigated by studying different rib profiles and GDL properties by modelling in order to decrease the lateral current density in the electrodes. It is possible that altering the cross-sectional shape of the rib from a square edge to a more rounded shape would have a beneficial effect, and this should be investigated.

The compression distribution in a stack was also studied. A model of a 5-cell stack was built based on an existing design. According to the model, the compression directed at the cells was highly uneven, with the corners of the active area under high compression and the centre parts experiencing less than 2 bars of compression pressure. This can be considered less than optimal as, according to other studies, good cell performance requires 10–15 bars of compression, though this value depends on the GDL material. Thus, the stack end plates were redesigned using a ribbed structure that allowed the mass of the end plates to be decreased while simultaneously increasing their rigidity. A further mass decrease was accomplished by changing the end plate material from steel to aluminium. The force applied to the nuts and bolts of the end plates was varied so that the corners had less torque, which also helped to even the compression distribution. The end result was that the new end plate and the bolt-specific forces produced the desired compression distribution in the 10–15 bar range. The model was experimentally validated by ex-situ measurements using a pressure-sensitive film. The measurement accuracy of the experiments suffered from high manufacturing tolerance of the cell components, but qualitatively the results are in agreement.

The results of the compression distribution study demonstrate that stack endplates need to be designed with care or the compression on the cells can be far from optimal, thus affecting the cell performance negatively. Modelling is an effective tool for determining an acceptable end plate structure. The compression modelling in this work has been continued by others. The model has been developed further employing thin, perforated flexible layers to even out the compression further. Thermal stresses were also included, although these were found to be insignificant. In the future, this model could be improved by adding more geometrical details and increasing the number of cells as the available computing capacity is increased.

The flow field of a free-breathing fuel cell was also modelled in this work. The performance of a free-breathing fuel cell depends strongly on the effectiveness of the natural convection in transferring oxygen to the cell and removing the reaction product water. This problem has been modelled using various assumptions and simplifications. In this work, the aim was to develop a computationally light yet reliable 3D model of a free-breathing fuel cell and then to use it to demonstrate the potential of such a model. Modelling the flow field of a free-breathing fuel cell is different to making the usual cell model, as the ambient air zone has to be included. This increases the size of the model and thus requires

more computing power. In order to find out how large the modelled ambient air zone should be, different sized zones with different types of boundary conditions were tested in 2D. These results were used in the building of a 3D model of a small 1 cm^2 cell. This model was then used to test how the position, i.e., tilt angle, of the cell and doubling the cell size affected performance. The results were that, as experiments have shown, a vertical alignment works best and increasing the cell size has no significant effect on its performance in this size range, though it can be expected that, at some point, increasing the cell size will create mass transport problems when the natural convection is no longer sufficient.

Mass transport was also modelled in the case of a free-breathing fuel cell. The model consisted of the cathode GDL and current collectors of the cell and the ambient air zone surrounding the cell. The model was 3D, but suitable boundary conditions and the correct size of the ambient air zone were first studied using a 2D model. The 3D model, built using the data from the 2D model, is computationally lighter than the free-breathing PEMFC models typically used but no less accurate. This model was used to perform some preliminary tests on the effect of the size and positioning of the cell on its performance. The result was that when the size of the cell is in the range of a few square centimetres, natural convection is effective in supplying the cell with reactants, and increasing the cell size does not have a strong effect on the cell behaviour.

The flow field and the model of the free-breathing fuel cell require the inclusion of two-phase phenomena to give good predictions however. At the time of writing this thesis, there simply are no reliable parameters for modelling two-phase phenomena in fuel cells. Even if the parameters widely used in fuel cell modelling were to be incorporated into this model, there would still be a problem of how to model the two-phase phenomena on the GDL/ambient air zone boundary where evaporation takes place. Excess water can also form droplets on this surface. In order to develop free-breathing fuel cell models or fuel cell models in general, further, reliable two-phase parameters should be derived either experimentally or theoretically, and suitable boundary conditions, semi-empirical correlations if necessary, should be developed.

This thesis is a study of different aspects of fuel cell operation connected together by the method of using modelling as a tool. As always in modelling, each model could have been developed further, but the line must be drawn somewhere and the length and depth of this work were determined by the practical constraints of each project of which the studies were made a part. In terms of future work, the most important improvements would be to add geometrical

details and complexity to the stack models and two-phase phenomena to the cell models. If computing capacity continues to increase, as it has done in the past, it will be possible one day to develop a model that combines most of the models in this study. This model would consist of the GDLs, MEA and flow channels of an entire cell and include contact resistance effects combined with flow field simulation and the results of a stack compression model. This model could show what kind of current density or thermal distribution the combined effect of local cell phenomena and cell-scale variations in reactant concentration and compression would cause in a fuel cell.

References

[1] http://www.epsomandewellhistoryexplorer.org.uk/Schonbein.html, last referred to on 16.11.2010

[2] F. Barbir, PEM Fuel Cells: Theory and Practise, Elsevier (2005)

[3] http://aboutfuelcells.wordpress.com/2007/06/04/ludwig-mond-and-charles-langer, last referred to on 16.11.2010

[4] http://www.ieeeghn.org/wiki/index.php/Bacon's_Fuel_Cell, last referred to on 16.11.2010

[5] http://www.fctec.com/fctec_history.asp, last referred to on 16.11.2010

[6] http://en.wikipedia.org/wiki/Gemini_V, last referred to on 16.11.2010

[7] Smithsonian institute http://scienceservice.si.edu/pages/059026.htm, last referred to on 4.12.2009

[8] http://www.hydrogencarsnow.com/blog2/index.php/hydrogenbus es/bc-transit-fuel-cell-buses-in-operation-for-2010-winter-olympics/, last referred to on 14.4.2011

[9] European Union, Fuel Cells and Hydrogen Joint Technology Initiative, http://ec.europa.eu/research/fch/index_en.cfm?pg=back, last referred to on 1.2.2010

[10] G. Meng, G. Ma, Q. Ma, R. Peng and X. Liu, Ceramic membrane fuel cells based on solid proton electrolytes, *Solid State Ionics* 178, pp. 697–703 (2007)

[11] W. Dai, H. Wang, X. Yuan, J.J. Martin, D. Yang, J. Qiao and J. Ma, A review on water balance in the membrane electrode assembly of proton exchange membrane fuel cells, *Int. J. Hydrogen Energy* 34, pp. 9461–9478 (2009)

[12] M.S. Wilson, F.H. Garzon, K.E. Sickafus and S. Gottesfeld, Surface area loss of supported platinum in polymer electrolyte fuel cells, *J. Electrochem. Soc.* 140, pp. 2872–2877 (1993)

[13] X. Cheng, L. Chen, C. Peng, Z. Chen, Y. Zhang and Q. Fan, Catalyst microstructure examination of PEMFC membrane electrode assemblies vs. time, *J. Electrochem. Soc.* 151, pp. A48–A52 (2004)

[14] D.A. Stevens and J.R. Dahn, Thermal degradation of the support in carbon-supported platinum electrocatalysts for PEM fuel cells, *Carbon* 43, p. 179 (2005)

[15] A. Collier, H. Wang, X.Z. Yuan, J. Zhang and D.P. Wilkinson, Degradation of polymer electrolyte membranes, *Int. J. Hydrogen Energy* 31, p. 1838 (2006)

[16] J. Xie, D.L. Wood, D.M. Wayne, T.A. Zawodzinski, P. Atanassov and R.L. Borup, Durability of PEFCs at high humidity conditions, *J. Electrochem. Soc.* 152, p. A104 (2005)

[17] C. Chung, L. Kim, Y.W. Sung, J. Lee and J.S. Chung, Degradation mechanism of electrocatalyst during long-term operation of PEMFC, *Int. J. Hydrogen Energy* 34, pp. 8974–8981 (2009)

[18] E. Endoh, S. Terazono, H. Widjaja and Y. Takimoto, Degradation study of MEA for PEMFCs under low humidity conditions, *Electrochem. Solid-State Lett.* 7, pp. A209–A211 (2004)

[19] J. Xie, D.L. Wood, III, K.L. More, P. Atanassov and R.L. Borup, Microstructural Changes of Membrane Electrode Assemblies during PEFC durability testing at high humidity conditions, *J. Electrochem. Soc.* 152, pp. A1011–A1020 (2005)

[20] X.L. Wang, H.M. Zhanga, J.L. Zhang, H.F. Xu, Z.Q. Tian, J. Chen, H.X. Zhong, Y.M. Liang and B.L. Yi, Micro-porous layer with composite carbon black for PEM fuel cells, *Electrochimica Acta* 51, pp. 4909–4915 (2006)

[21] H. K. Atiyeh, K. Karan, B. Peppley, A. Phoenix, E. Halliop and J. Pharoah, Experimental investigation of the role of a microporous layer on the water transport and performance of a PEM fuel cell, *J. Power Sources* 170, pp. 111–121 (2007)

[22] M.H. Oha, Y.S. Yoon and S.G. Park, The electrical and physical properties of alternative material bipolar plate for PEM fuel cell system, *Electrochimica Acta* 50, Pp. 777–780 (2004)

[23] C. Hui, L. Hong-bo, Y. Li, L. Jian-xin and Y. Li, Study on the preparation and properties of novolac epoxy/graphite composite bipolar plate for PEMFC *Int. J. Hydrogen Energy* 35, pp. 3105–3109 (2010)

[24] E.A. Cho, U.-S. Jeon, S.-A. Hong, I-H. Oh and S.-G. Kang, Performance of a 1 kW-class PEMFC stack using TiN-coated 316 stainless steel bipolar plates, *J. Power Sources* 142, pp. 177–183 (2005)

[25] K. Lee, S. Lee, J. Kim, Y. Lee, Y. Kim, M. Kim and D. Wee, Effects of thermal oxi-nitridation on the corrosion resistance and electrical conductivity of 446M stainless steel for PEMFC bipolar plates, *Int. J. Hydrogen Energy* 34, pp. 1515–1521 (2009)

[26] S. Joseph, J.C. McClure, R. Chianelli, P. Pich and P.J. Sebastian, Conducting polymer-coated stainless steel bipolar plates for proton exchange membrane fuel cells (PEMFC), *Int. J. Hydrogen Energy* 30, pp. 1339–1344 (2005)

[27] J. Chen, Experimental study on the two phase flow behavior in PEM fuel cell parallel channels with porous media inserts, *J. Power Sources* 195, pp. 1122–1129 (2010)

[28] D.G. Strickland and J.G. Santiago, In situ polymerized wicks for passive water management in PEM fuel cells, *J. Power Sources* 195, pp. 1667–1675 (2010)

[29] J.S. Yi and T.V. Nguyen, Multicomponent transport in porous electrodes of proton exchange membrane fuel cells using the interdigitated gas distributors, *J. Electrochem. Soc.* 146, pp. 38–45 (1999)

[30] A. Kazim, H.T. Liu and P. Forges, Modelling of performance of PEM fuel cells with conventional and interdigitated flow fields, *J. Appl. Electrochem.* 29, pp. 1409–1416 (1999)

[31] A. Kumar and R.G. Reddy, Effect of channel dimensions and shape in the flow-field distributor on the performance of polymer electrolyte membrane fuel cells, *J. Power Sources* 113, pp. 11–18 (2003)

[32] H. Meng and C.Y. Wang, Large-scale simulation of polymer electrolyte fuel cells by parallel computing, *Chem Eng Sci* 59, pp. 3331–3343 (2004)

[33] Y. Yoon, W. Lee, G. Park, T. Yang and C. Kim, Effects of channel configurations of flow field plates on the performance of a PEMFC, *Electrochimica Acta* 50, pp. 709–712 (2004)

[34] S. Shimpalee and J.W. Van Zee, Numerical studies on rib & channel dimension of flow-field on PEMFC performance, *Int. J. Hydrogen Energy* 32, pp. 842–856 (2007)

[35] S.A. Vilekar and R. Datta, The effect of hydrogen crossover on open-circuit voltage (OCV) in PEM fuel cells, *J. Power Sources*, Accepted Manuscript (2009)

[36] M. Andersson, J. Yuan and B. Sundén, Review on modeling development for multiscale chemical reactions coupled transport phenomena in solid oxide fuel cells, *Applied Energy* 87, pp. 1461–1476 (2010)

[37] M.G. Santarelli, M.F. Torchio and P. Cochis, Parameters estimation of a PEM fuel cell polarization curve and analysis of their behavior with temperature, *J. Power Sources* 159, pp. 824–835 (2006)

[38] N. Djilali, Computational modelling of polymer electrolyte membrane (PEM) fuel cells, Challenges and opportunities, *Energy* 32, pp. 269–280 (2007)

[39] R. Madhusudana Rao and R. Rengaswamy, Dynamic characteristics of spherical agglomerate for study of cathode catalyst layers in proton exchange membrane fuel cells (PEMFC), *J. Power Sources* 158, pp. 110–123 (2006)

[40] D. Cheddie and N. Munroe, Review and comparison of approaches to proton exchange membrane fuel cell modelling, *J. Power Sources* 147, pp. 72–84 (2005)

[41] C. Siegel, Review of computational heat and mass transfer modeling in polymer-electrolyte-membrane (PEM) fuel cells, *Energy* 33, pp. 1331–1352 (2008)

[42] F. Standaert, K. Hemmes and N. Woudstra, Analytical fuel cell modeling, *J. Power Sources* 63, pp. 221–234 (1996)

[43] D. Bernardi and M. Verbrugge, A mathematical model of the solid polymer electrolyte fuel cell, *J. Electrochem. Soc.* (1992)

[44] M. Khakpour and K. Vafai, Analysis of transport phenomena within PEM fuel cells – An analytical solution, *Int. J. Heat and Mass Transfer* 51, pp. 3712–3723 (2008)

[45] D.F. Cheddie and N.D.H. Munroe, Semi-analytical proton exchange membrane fuel cell modelling, *J. Power Sources* 183, pp. 164–173 (2008)

[46] T.E. Springer, T.A. Zawodzinski and S. Gottesfeld, Polymer electrolyte fuel cell model, *J. Electrochem. Soc.* 138, pp. 2334–2342 (1991)

[47] H. Huisseune, A. Willockx and M. De Pepe, Semi-empirical along-the-channel model for a proton exchange membrane fuel cell, *Int. J. Hydrogen Energy* 33, pp. 6270–6280 (2008)

[48] L. Pisani, G. Murgia, M. Valentini and B. D'Aguanno, A new semi-empirical approach to performance curves of polymer electrolyte fuel cells, *J. Power Sources* 108, pp. 192–203 (2002)

[49] M.A.R. Sadiq Al-Baghdadi, Modelling of proton exchange membrane fuel cell performance based on semi-empirical equations, *Renewable Energy* 30, pp. 1587–1599 (2005)

[50] T.E. Springer, T.A. Zawodzinski and S. Gottesfeld, Polymer electrolyte fuel cell model, *J Electrochem Soc* 138, pp. 2334–2342 (1991)

[51] D.M. Bernardi and M.W. Verbrugge, Mathematical model of a gas diffusion electrode bonded to a polymer electrolyte, *AIChE J.* 37, pp. 1151–1163 (1991)

[52] D. Singh, D. Lu and N. Djilali, A two-dimensional analysis of mass transport in proton exchange membrane fuel cells, *Int. J. Eng. Sci* 37, pp. 431–452 (1999)

[53] T.V. Nguyen and R.E. White, A water and heat management model for proton-exchange-membrane fuel cells. *J. Electrochem. Soc.* 140, pp. 2178–2186 (1993)

[54] S. Dutta, S. Shimpalee and J.W. van Zee, Three-dimensional numerical simulation of straight channel PEM fuel cells, *J Appl Electrochem* 30, pp. 135–146 (2000)

[55] S. Dutta, S. Shimpalee and J.W. van Zee, Numerical prediction of mass-exchange between cathode and anode channels in a PEM fuel cell, *Int J Heat Mass Transfer* 44, pp. 2029–2042 (2001)

[56] T. Berning, D.M. Lu and N. Djilali, Three-dimensional computational analysis of transport phenomena in PEM fuel cells, *J Power Sources* 106, pp. 284–294 (2002)

[57] A. Kumar and R.G. Reddy, Effect of the channel dimensions and shape in the flow field distributor on the performance of polymer electrolyte membrane fuel cells, *J Power Sources* 113, pp. 11–18 (2003)

[58] G. Mmaranzana, C. Moyne, J. Dillet, S. Didierjean and O. Lottin, About internal currents during start-up in PEMFC, *J. Power Sources* 195, pp. 5990–5995 (2010)

[59] P.R. Pathapati, X. Xue and J. Tang, A new dynamic model for predicting transient phenomena in a PEM fuel cell system, *Renewable Energy* 30, pp. 1–22 (2005)

[60] N. Wagner, Characterization of membrane electrode assemblies in polymer electrolyte fuel cells using a.c. impedance spectroscopy, *J. App. Electrochem.* 32, pp. 859–863 (2002)

[61] T.-W. Lee, J. Hur, B.-K. Lee and C.-Y. Won, Design of a fuel cell generation system using a PEMFC simulator, *Electric Power Systems Research* 77, pp. 1257–1264 (2007)

[62] M. Ceraolo, C. Miuli and A. Pozio, Modelling static and dynamic behaviour of proton exchange membrane fuel cells on the basis of the electro-chemical description, *J. Power Sources* 113, pp. 131–144 (2003)

[63] S. Yerramalla, A. Davari, A. Feliachi and T. Biswas, Modeling and simulation of the dynamic behavior of a polymer electrolyte membrane fuel cell, *J. Power Sources* 124, pp. 104–113 (2003)

[64] Z.H. Wang, C.Y. Wang and K.S. Chen, Two-phase flow and transport in the air cathode of proton exchange membrane fuel cells, *J. Power Sources* 94, 15, pp. 40–50 (2001)

[65] L. You and H. Liu, A two-phase flow and transport model for the cathode of PEM fuel cells, *Int. J. Heat and Mass Transfer* 45, pp. 2277–2287 (2002)

[66] U. Pasaogullari and C. Wang, Two-phase modeling and flooding prediction of polymer electrolyte fuel cells, *J. Electrochem. Soc.* 152, pp. A380–A390 (2005)

[67] D. Natarajan and T.V. Nguyen, A two-dimensional, two-phase, multicomponent, transient model for the cathode of a proton exchange membrane fuel cell using conventional gas distributors, *J. Electrochem. Soc.* 148, pp. A1324–A1335 (2001)

[68] T. Berning, D.M. Lu and N. Djilali, Three-Dimensional Computational Analysis of Transport Phenomena in a PEM Fuel Cell, *J. Power Sources* 106, pp. 284–294 (2002)

[69] T. Kim, J. Kim, C. Sim, S. Lee, M. Kaviany, S. Young Son and M. Kim, Experimental approaches for distribution and behavior of water in PEMFC under flow direction and differential pressure using neutron imaging technique, *Nuclear Instruments and Methods in Physics Research Section A: Accelerators, Spectrometers, Detectors and Associated Equipment* 600. Pp. 325–327 (2009)

[70] C. Min, A novel three-dimensional, two-phase and non-isothermal numerical model for proton exchange membrane fuel cell, *J. Power Sources* 195, pp. 1880–1887 (2009)

[71] T. Ous and C. Arcoumanis, Visualisation of water droplets during the operation of PEM fuel cells, *J. Power Sources* 173, pp. 137–148 (2007)

[72] T. Berning, M. Odgaard and S.K. Kær1, A Computational Analysis of Multiphase Flow Through PEMFC Cathode Porous Media Using the Multifluid Approach, *J. Electrochem. Soc.* 156, pp. B1301–B1311 (2009)

[73] V. Gurau, T.A. Zawodzinski Jr., J.A. Mann Jr., Two-phase transport in PEM fuel cell cathodes, *J. Fuel Cell Sci. Technol.* 5, (2008)

[74] S. Larsson and V. Thomée, Partial Differential Equations with Numerical Methods, Springer (2005)

[75] R. Taylor and R. Krishna, Multicomponent mass transfer, Wiley (1993)

[76] N. Akhtar, A. Qureshi, J. Scholta, C. Hartnig, M.S. Messerschmidt and W. Lehnert, Investigation of water droplet kinetics and optimization of channel geometry for PEM fuel cell cathodes, *Int. J. of Hydrogen Energy* 34, pp. 3104–3111 (2009)

[77] J. Scholta, G. Escher, W. Zhang, L. Küppers, L. Jörissen and W. Lehnert, Investigation on the influence of channel geometries on PEMFC performance, *J. Power Sources* 155, pp. 66–71 (2006)

[78] G. He, Y. Yamazaki, and A. Abudula, A droplet size dependent multiphase mixture model for two phase flow in PEMFCs, *J. Power Sources* 194, pp. 190–198 (2009)

[79] X. Li and I. Sabir, Review of bipolar plates in PEM fuel cells: Flow-field designs, *Int. J. Hydrogen Energy* 30, pp. 359–371 (2005)

[80] J. Ihonen, F. Jaouen, G. Lindbergh and G. Sundholm, A novel polymer electrolyte fuel cell for laboratory investigations and in-situ contact resistance measurements, *Electrochim. Acta* 46, pp. 2899–2911 (2001)

[81] V. Mishra, F. Yang and R. Pitchumani, Measurement and prediction of electrical contact resistance between gas diffusion layers and bipolar plate for applications to PEM fuel cells, *J. Fuel Cell Sci. Technol.* 1, pp. 2–9 (2004)

[82] I. Nitta, T. Hottinen, O. Himanen and M. Mikkola, Inhomogeneous compression of PEMFC gas diffusion layer. Part I. Experimental, *J. Power Sources* 171, pp. 26–36 (2007)

[83] I. Nitta, O. Himanen and M. Mikkola, Contact resistance between gas diffusion layer and catalyst layer of PEM fuel cell, *Electrochem. Comm.* 10, pp. 47–51 (2008)

[84] J. Ihonen, M. Mikkola and G. Lindbergh, Flooding of Gas Diffusion Backing in PEFCs, *J. Electrochem. Soc.* 151, pp. A1152–A1161 (2004)

[85] S. Escribano, J.-F. Blachot, J. Ethève, A. Morin and R. Mosdale, Characterization of PEMFCs gas diffusion layers properties, *J. Power Sources* 156, pp. 8–13 (2006)

[86] W. Lee, C.-H. Ho, J.W. Van Zee and M. Murthy, The effects of compression and gas diffusion layers on the performance of a PEM fuel cell, *J. Power Sources* 84, pp. 45–51 (1999)

[87] M. Mikkola, T. Tingelöf and J. Ihonen, Modelling compression pressure distribution in fuel cell stacks, *J. Power Sources* 193, pp. 269–275 (2009)

[88] M. Mikkola and P. Koski, Modeling the internal pressure distribution of a fuel cell, *COMSOL Conference 2009, Milan, Italy, October 14–16, 2009*, Proceedings of the Comsol Conference (2009)

[89] S. Litster, J.G. Pharoah, G. McLeana and N. Djilali, Computational analysis of heat and mass transfer in micro-structured PEMFC cathode, *J. Power Sources* 156, pp. 334–344 (2006)

[90] P. Manoj Kumar and A.K. Kolar, Effect of cathode design on the performance of an air-breathing PEM fuel cell, *J. Power Sources* 35, pp. 671–681 (2010)

[91] M. Havet and D. Blay, Natural convection over a non-isothermal vertical plate, *Int. J. Heat and Mass Transfer* 42, pp. 3103–3112 (1999)

[92] S. Pretot, B. Zeghmati and G. Le Palec, Theoretical and experimental study of natural convection on a horizontal plate, *Applied Thermal Engineering* 20, pp. 873–891 (2000)

Appendix A: Parameter Correlations and Constants

Parameter Correlations

Parameter name	Equation	Publi-cation
Heat production rate	$q_0 = i\left(\eta + \frac{326T}{4F}\right)\cdot 0.8$	5
Water production rate	$\dot{\mathbf{N}}_{H2O} = -\frac{i}{2F} M_{H2O}$	1,2,3,5
Oxygen consumption rate	$\dot{\mathbf{N}}_{O2} = \frac{i}{4F} M_{O2}$	1,2,3,5
Reynold's number	$\mathrm{Re} = \frac{\rho u D_h}{\eta}$	1
Effective diffusion coefficient	$D^{\mathrm{eff}} = D(\varepsilon(1-s))^{1.5}$	2,3,5
Average density of air	$\rho(s) = \frac{(p_{\mathrm{atm}} + p)(M_{\mathrm{H_2O}} x_{\mathrm{H_2O}}(s) + M_{\mathrm{O_2}} x_{\mathrm{O_2}}(s) + M_{\mathrm{N_2}} x_{\mathrm{N_2}} + M_{\mathrm{Ar}} x_{\mathrm{Ar}})}{RT}$	1,2,3,5
Average viscosity of air	$\eta_{air}(s) = \left(\frac{x_{\mathrm{H_2O}}(s)}{\eta_{\mathrm{H_2O}}} + \frac{x_{\mathrm{O_2}}(s)}{\eta_{\mathrm{O_2}}} + \frac{x_{\mathrm{N_2}}}{\eta_{\mathrm{N_2}}} + \frac{x_{\mathrm{Ar}}}{\eta_{\mathrm{Ar}}}\right)^{-1} \cdot \frac{\rho(s)}{\rho_{\mathrm{in}}}$	1,2,3,5
Binary diffusion coefficients	$D_{ij} = C\frac{T^{1.75}\sqrt{1/M_i + 1/M_j}}{p\left((v_i)^{1.3} + (v_j)^{1.3}\right)^2}$ or alternatively $D_{i,j} = \frac{p_0}{p}\left(\frac{T}{T_0}\right)^{1.5} D_{i,j}(p_0, T_0)$	1,2,3,5

Heat production in the cell	$q_0 = i\left(\eta_c + \frac{326T}{4F}\right)\cdot 0.8$	5
Exchange current density on the cathode	$i_0(T) = i_0(T_0)\exp\left(-\frac{\Delta E}{R}\left(\frac{1}{T}-\frac{1}{T_0}\right)\right)$	5
Saturation molar fraction	$X_{sat} = \frac{p_{sat}}{p}$	1,2,3
Saturation pressure	$\log(p_{sat}) = 28.59051 - 8.2\log(T+0{,}01) + 0.0024804(T+0.01) - 3142.31/(T+0.01)$	1,2,3
Maxwell–Stefan diffusion coefficients	$D_{11} = D_{O_2,N_2}\frac{X_{O_2}D_{H_2O,N_2} + (1-X_{O_2})D_{O_2,H_2O}}{S}$ $D_{12} = X_{O_2}D_{H_2O,N_2}\frac{D_{O_2,N_2} - D_{O_2,H_2O}}{S}$ $D_{21} = X_{H_2O}D_{O_2,N_2}\frac{D_{H_2O,N_2} - D_{O_2,H_2O}}{S}$ $D_{22} = D_{H_2O,N_2}\frac{X_{H_2O}D_{O_2,N_2} + (1-X_{H_2O})D_{O_2,H_2O}}{S}$ $S = X_{O_2}D_{H_2O,N_2} + X_{H_2O}D_{O_2,N_2} + X_{N_2}D_{O_2,H_2O}$	1,2,3,5

Constants

The properties of dry standard air used in Publications 1, 2, 3 and 5

Component	*Molar mass* ($gmol^{-1}$)	*Molar fraction in air*	*Viscosity η at 343 K (Pas)*	*Density ρ at 343 (K kgm^{-3})*	*Diffusion volume v (m^3mol^{-1})*
Nitrogen	28	0.78	$1.97\cdot10^{-5}$	0.995	$12.7\cdot10^{-6}$
Oxygen	32	0.21	$2.29\cdot10^{-5}$	1.137	$16.6\cdot10^{-6}$
Argon	40	0.1	$2.60\cdot10^{-5}$	1.421	-
Water	18	0	$1.15\cdot10^{-5}$	0.64	$17.9\cdot10^{-6}$

The mechanical properties of materials used in Publication 4

Component	*E (GPa)*	*υ*
Flow field plate (graph/epoxy)	10	0.25
Gas diffusion layer	0.06	0.33
Grafoil	1.4	0.25
Steel	200	0.33
Aluminium	70	0.33
Rubber	0.1	0.4
Steel net	110	0.33

Various constants used in the models

Constant	*Explanation*	*Value*
$a_v j_a^{ref}$	Exchange current density × ratio of reaction surface to CL volume, anode (2D)	1.7×10^9 A m^{-3}
$a_v j_c^{ref}(T_0)$	Exchange current density × ratio of reaction surface to CL volume, cathode (2D)	2×10^4 A m^{-3}
$\alpha_a^a + \alpha_c^a$	Anodic and cathodic transfer coefficients	1
α	Water transfer coefficient	0.5
C_{p,O_2}	Heat capacity of oxygen	923 J kg^{-1} K^{-1}
C_{p,H_2O}	Heat capacity of water	1996 J kg^{-1} K^{-1}
c_p	Heat capacity of air	1005.38007 J/kg K
c_{cc}	Heat capacity of the current collector	1000 J/kg K
C	Diffusion coefficient constant	$3.16 \cdot 10^{-8}$
$c_{O2,0}$	Oxygen concentration in ambient air	8.39128 mol/m^3
c_{H2O0}	Water concentration in ambient air	0.403621 mol/m^3
$D_{O_2,H_2O}(p_0,T_0)$	Binary diffusion coefficient O_2,H_2O	3.98×10^{-5} m^2 s$^-$
$D_{O_2,N_2}(p_0,T_0)$	Binary diffusion coefficient O_2,N_2	2.95×10^{-5} m^2 s^{-1}
$D_{H_2O,N_2}(p_0,T_0)$	Binary diffusion coefficient H_2O,N_2	4.16×10^{-5} m^2 s^{-1}

E_0	Open circuit voltage	1.23 V
ΔE_{exc}	Activation energy	($E_{cell} \geq 0.8V$) 76.5 kJ mol^{-1} ($E_{cell} < 0.8V$) 27.7 kJ mol^{-1}
ε_0	Porosity of uncompressed GDL	0.83
ε_{CL}	Porosity of CL	0.4
η_c	Activation overpotential	0.6 V
F	Faraday's constant	96485 C/mol
g	Gravitational acceleration	9.81 m/s^2
$i_0(T_0)$	Exchange current density	0.01 A/m^2
k	Heat conductivity of air	0.026044 J/m^2
k_{GDL}	Effective heat conductivity of the GDL	0.3 W/m
κ_{CL}	CL thermal conductivity	0.476 W m^{-1} K^{-1}
κ_{GDL}	GDL thermal conductivity	1.18
k_{cc}	Thermal conductivity of the current collector	14 J/m^2
κ	GDL permeability	$2.06 \cdot 10^{-12}$ m^2
σ_{GR}	Graphite plate electric conductivity	69700 S m^{-1}
κ_{GR}	Graphite plate thermal conductivity	128 W m^{-1} K^{-1}
σ_m	Membrane ionic conductivity	5.09 S m^{-1}
κ_m	Membrane thermal conductivity	0.12 W m^{-1} K^{-1}
κ_h	Heat transfer coefficient from GDL to air	5 W m^{-2} K^{-1}
k_{CL}	Permeability of CL	1.26×10^{-13} m^2
p_0	Ambient pressure	10^5 Pa
R	Universal gas constant	8.314 J/mol K
ΔS_c	Entropy change of cathode	326.36 J mol^{-1} K^{-1}
ΔS_a	Entropy change of anode	0.104 J mol^{-1} K^{-1}
σ_s^{CL}	CL electric conductivity	320 S m^{-1}
σ_m^{CL}	CL ionic conductivity	5.09 S m^{-1}
T_0	Reference temperature	273 K

Appendix B: Publications 1–5

Series title, number and
report code of publication

VTT Publications 772
VTT-PUBS-772

Author(s)
Suvi Karvonen

Title

Modelling approaches to mass transfer and compression effects in polymer electrolyte fuel cells

Abstract

The subject of the thesis is modelling polymer electrolyte membrane fuel cells (PEMFCs) locally and on a cell scale. The modelling was done using software based on the finite element method and focused on mass transfer issues and compression pressure distribution and its effects on local phenomena.

Mass transfer, more specifically the flow distribution in the flow field system, was studied on the cathode. The velocity distribution was improved by changing the geometry of the channel system. This improvement was also observed experimentally. Mass transport problems of free-breathing fuel cells were also studied. These cells rely on free convection to provide reactants and remove reaction products. In this thesis, the aim was to develop an accurate model that is also computationally light.

The compression distribution in a stack was modelled based on an existing stack design. The results showed poor internal pressure distribution, with most of the cell experiencing insufficient compression. The modelling was then used to find a better end plate structure and suitable torques for the nut and bolt assemblies. The results were validated experimentally.

The effect of compression was studied on a local scale on which compression variations caused by the channel structure had been seen to affect the gas diffusion layer properties and contact resistances between components. According to the modelling results, there are strong local transversal electric currents in the cell. This phenomenon can affect the cell performance and lifetime negatively.

ISBN
978-951-38-7754-5 (soft back ed.)
978-951-38-7755-2 (URL: http://www.vtt.fi/publications/index.jsp)

Series title and ISSN	Project number
VTT Publications 1235-0621 (soft back ed.) 1455-0849 (URL: http://www.vtt.fi/publications/index.jsp)	

Date	Language	Pages
October 2011	English, Finnish abstr.	73 p. + app. 66 p.

Name of project	Commissioned by

Keywords	Publisher
PEMFC, fuel cell, modelling	VTT Technical Research Centre of Finland P.O. Box 1000, FI-02044 VTT, Finland Phone internat. +358 20 722 4520 Fax +358 20 722 4374

Julkaisun sarja, numero ja raporttikoodi

VTT Publications 772
VTT-PUBS-772

Tekijä(t)
Suvi Karvonen

Nimeke

Polymeerielektrolyyttipolttokennojen massansiirron ja puristuspaineen vaikutusten mallintaminen

Tiivistelmä

Väitöskirja käsittelee polymeerielektrolyyttipolttokennon (PEMFC) toiminnan mallinnusta paikallisesti ja kennotasolla. Tutkimuksen työkaluna on käytetty mallinnusta elementtimenetelmään perustuvalla ohjelmistolla. Mallinnuksen painopisteinä ovat erityisesti aineensiirron ongelmat ja puristuspaineen jakautuminen ja vaikutus kennon paikalliseen toimintaan.

Aineensiirtoa eli virtauskanaviston toimintaa tarkasteltiin kennon katodilla mallintamalla kanavistoon syntyvää virtausprofiilia. Kanaviston geometriaa muuttamalla pystyttiin parantamaan virtausprofiilia, ja tämä mallinnuksen avulla suoritettu optimointi havaittiin myös kokeellisesti. Aineensiirron kysymyksiä tutkittiin myös vapaasti hengittävien polttokennojen kohdalla. Näissä kennoissa aineensiirto perustuu vapaaseen konvektioon. Työssä pyrittiin kehittämään yhtä aikaa luotettava ja laskennallisesti kevyt malli. Lopputuloksena syntyi kolmiulotteinen malli vapaasti hengittävästä kennosta, jolla tutkittiin kennon koon ja asennon vaikutusta toimintaan.

Kennostossa vallitsevaa puristuspainetta mallinnettiin olemassa olevaan kennostoon perustuvan mekaanisen mallin avulla. Tuloksena saatiin epätasainen painejakauma. Mallinnuksen avulla etsittiin parempi rakenne kennoston päätylevyille sekä muutettiin pulttien vääntömomentteja, jolloin kennolla vallitseva painejakauma saatiin pysymään toivotuissa rajoissa. Samalla päätylevyn painoa saatiin vähennettyä. Tulokset verifioitiin kokeellisesti.

Puristuspaineen vaikutusta tutkittiin paikallisella tasolla, jossa virtauskanaviston rakenteen aiheuttamien painevaihteluiden oli todettu vaikuttavan merkittävästi kaasudiffuusiokerrosten ominaisuuksiin ja komponenttien välisiin resistansseihin. Mallinnuksen tulosten mukaan kennossa syntyy paikallisesti merkittävästi poikittaissuuntaista sähkövirtaa, joka aiheuttaa virrantiheyteen vaihteluja. Ilmiö voi vaikuttaa negatiivisesti kennon toimintaan ja elinikään.

ISBN
978-951-38-7754-5 (nid.)
978-951-38-7755-2 (URL: http://www.vtt.fi/publications/index.jsp)

Avainnimeke ja ISSN	Projektinumero
VTT Publications 1235-0621 (nid.) 1455-0849 (URL: http://www.vtt.fi/publications/index.jsp)	

Julkaisuaika	Kieli	Sivuja
Lokakuu 2011	Suomi, engl. tiiv.	73 s. + liitt. 66 s.

Projektin nimi	Toimeksiantaja(t)

Avainsanat	Julkaisija
PEMFC, fuel cell, modelling	VTT PL 1000, 02044 VTT Puh. 020 722 4520 Faksi 020 722 4374

The subject of this thesis is modelling polymer electrolyte membrane fuel cells (PEMFCs), with the focus on mass transfer and compression pressure distribution issues. Good understanding of these subjects is necessary for improving PEMFC lifetime and performance and eventually making them viable for wide scale commercial applications.

Mass transfer on the cathode was shown to be improved by certain changes to the geometry of the channel system and also studied in the case of a free-breathing fuel cell. A similar improvement was found concerning the compression distribution through making changes to geometry and torques. The effect of compression was also studied on a local scale, showing how the channel structure causing uneven contact resistances can lead to unexpected local current distributions.

ISBN 978-951-38-7754-5 (soft back ed.)
ISSN 1235-0621 (soft back ed.)

ISBN 978-951-38-7755-2 (URL: http://www.vtt.fi/publications/index.jsp)
ISSN 1455-0849 (URL: http://www.vtt.fi/publications/index.jsp)